

# Environmental Sustainability

## Nodulation in the absence of nod genes induction: alternative mechanisms involved in the symbiotic interaction between Cupriavidus sp. UYMMa02A and Mimosa pudica --Manuscript Draft--

<b>Manuscript Number:</b>	ENVS-D-22-00162R3	
<b>Full Title:</b>	Nodulation in the absence of nod genes induction: alternative mechanisms involved in the symbiotic interaction between Cupriavidus sp. UYMMa02A and Mimosa pudica	
<b>Article Type:</b>	Original Article	
<b>Funding Information:</b>	Agencia Nacional de Investigación e Innovación (FCE_1_2014_1_104338)	Dr. Raúl Alberto Platero
	Agencia Nacional de Investigación e Innovación (FCE_1_2017_1_136082)	Dr. Raúl Alberto Platero
	Agencia Nacional de Investigación e Innovación (FCE_1_2019_1_156520)	Dr. Raúl Alberto Platero
	Programa de desarrollo de las ciencias básicas, PEDECIBA (2018)	Not applicable
	FONTAGRO (ID 30)	Dr. Raúl Alberto Platero
<b>Abstract:</b>	<p>Abstract: Cupriavidus sp. UYMMa02A is a beta-rhizobia strain of the Cupriavidus genus, isolated from nodules of Mimosa magentea in Uruguay. This strain can form effective nodules with several Mimosa species, including its original host. Genome analyses indicate that Cupriavidus sp. UYMMa02A has a highly conserved 35kb symbiotic island containing nod, nif, and fix operons, suggesting conserved mechanisms for the symbiotic interaction with plant hosts. However, while Cupriavidus sp. UYMMa02A produces functional nodules and promotes Mimosa pudica growth under nitrogen-limiting conditions, nod genes are not induced by luteolin or exposure to Mimosa spp. root exudate. To explore alternative mechanisms implicated in the Cupriavidus-Mimosa interaction, we assessed the proteomic profiles of Cupriavidus sp. UYMMa02A grown in the presence of pure flavonoids and co-culture with Mimosa pudica plants. This approach allowed us to identify 24 differentially expressed proteins potentially involved in bacterial-plant interaction. In light of the obtained results, a possible model for nod-alternative symbiotic interaction is proposed.</p>	
<b>Corresponding Author:</b>	Raúl Alberto Platero, Ph Instituto de Investigaciones Biológicas Clemente Estable Montevideo, Montevideo URUGUAY	
<b>Corresponding Author Secondary Information:</b>		
<b>Corresponding Author's Institution:</b>	Instituto de Investigaciones Biológicas Clemente Estable	
<b>Corresponding Author's Secondary Institution:</b>		
<b>First Author:</b>	María Cecilia Rodríguez-Esperón, MSc	
<b>First Author Secondary Information:</b>		
<b>Order of Authors:</b>	María Cecilia Rodríguez-Esperón, MSc	
	Laura Sandes, MSc	
	Ignacio Eastman	
	Carolina Croci	
	Florencia Garabato	
	Virginia Ferreira, PhD	

	Martín Baraibar, PhD
	Magdalena Portela, PhD
	Rosario Durán, PhD
	Raúl Alberto Platero, PhD
<b>Order of Authors Secondary Information:</b>	
<b>Author Comments:</b>	<p>We have addressed all the comments made by the editor.</p> <p>We have removed figures and tables mentioned in the Discussion section.</p> <p>We have thoroughly checked the manuscript and removed grammatical errors. Some sentences were rephrased for improved comprehension.</p>
<b>Response to Reviewers:</b>	<p>We thank the reviewers for their work. For writing the current version we had taken into account all the reviewer's comments and suggestions. We have carefully reviewed English style and grammar. The result is an enhanced manuscript version that we think fulfills the requirements for being considered to be published in Environmental Sustainability.</p>

[Click here to view linked References](#)

1     1     **Nodulation in the absence of *nod* genes induction: alternative mechanisms**  
2  
3     2     **involved in the symbiotic interaction between *Cupriavidus* sp. UYMMa02A**  
4  
5     3     **and *Mimosa pudica*.**

6  
7  
8  
9     4     **Abstract:** *Cupriavidus* sp. UYMMa02A is a beta-rhizobia strain of the  
10  
11     5     *Cupriavidus* genus, isolated from nodules of *Mimosa magentea* in Uruguay. This  
12  
13     6     strain can form effective nodules with several *Mimosa* species, including its  
14  
15     7     original host. Genome analyses indicate that *Cupriavidus* sp. UYMMa02A has a  
16  
17     8     highly conserved 35kb symbiotic island containing *nod*, *nif*, and *fix* operons,  
18  
19     9     suggesting conserved mechanisms for the symbiotic interaction with plant hosts.  
20  
21  
22     10    However, while *Cupriavidus* sp. UYMMa02A produces functional nodules and  
23  
24     11    promotes *Mimosa pudica* growth under nitrogen-limiting conditions, *nod* genes  
25  
26     12    are not induced by luteolin or exposure to *Mimosa* spp. root exudate. To explore  
27  
28     13    alternative mechanisms implicated in the *Cupriavidus*-*Mimosa* interaction, we  
29  
30     14    assessed the proteomic profiles of *Cupriavidus* sp. UYMMa02A grown in the  
31  
32     15    presence of pure flavonoids and co-culture with *Mimosa pudica* plants. This  
33  
34     16    approach allowed us to identify 24 differentially expressed proteins potentially  
35  
36     17    involved in bacterial-plant interaction. In light of the obtained results, a possible  
37  
38     18    model for *nod*-alternative symbiotic interaction is proposed.  
39  
40  
41  
42  
43  
44  
45  
46  
47     19

## 20 Introduction

21 Rhizobia are soil bacteria that engage in symbiotic interactions with legume  
22 plants. During this interaction, new specialized organs called nodules are formed  
23 in the roots (and sometimes in stems) of host plants. Inside the nodules, bacteria  
24 convert atmospheric nitrogen into ammonia in a process known as Symbiotic  
25 Nitrogen Fixation (SNF) (Lindström and Mousavi, 2020).

26 The ability to form nitrogen-fixing nodules in symbiosis with legumes is restricted  
27 to alpha and beta subgroups of proteobacteria (Andrews and Andrews, 2017).

28 The best-characterized rhizobia species; *Sinorhizobium meliloti*, *Rhizobium*  
29 *leguminosarum*, or *Bradyrhizobium japonicum*, belong to the *Rhizobiaceae* family  
30 of alpha-proteobacteria. In beta-proteobacteria, the *Burkholderiaceae* family is  
31 the best characterized and includes just three genera *Paraburkholderia*, *Trinickia*,  
32 and *Cupriavidus* (Chen et al., 2001, 2003; Dall’Agnol et al., 2017; Estrada-de los  
33 Santos et al., 2018)(3–6). Both *Paraburkholderia* and *Cupriavidus* rhizobia strains  
34 were described at the beginning of the 21<sup>st</sup> century. Since then, beta-rhizobia  
35 have been described as legume symbionts in America (Bontemps et al.; Andam  
36 et al., 2007; dos Reis et al., 2010; Taulé et al., 2012), Africa (Garau et al., 2009;  
37 Howieson et al., 2013; Lemaire et al., 2015), Asia (Liu et al., 2012; Gehlot et al.,  
38 2013) and Oceania (Parker et al., 2007), primarily associated with legumes of  
39 Mimosoid clade, but also with some members of the *Papilionoideae* (Garau et al.,  
40 2009; Lemaire et al., 2015). Despite their worldwide distribution, the molecular  
41 mechanisms involved in the interaction between beta-rhizobia and host plants  
42 have been analyzed in a few model strains (Amadou et al., 2008; de Campos et  
43 al., 2017; Lardi et al., 2017; Klonowska et al., 2018; Bellés-Sancho et al., 2022;

1  
2  
3  
4  
5  
6  
7  
8  
9  
10  
11  
12  
13  
14  
15  
16  
17  
18  
19  
20  
21  
22  
23  
24  
25  
26  
27  
28  
29  
30  
31  
32  
33  
34  
35  
36  
37  
38  
39  
40  
41  
42  
43  
44  
45  
46  
47  
48  
49  
50  
51  
52  
53

Rodríguez-Esperón et al., 2022). Genome analyses of beta-rhizobia that nodulate Mimosoid clade have shown the presence of a highly conserved and compact genomic region, known as the symbiotic island, that encodes for *nod*, *nif*, and *fix* genes (Sofie E. De Meyer et al., 2016; Zheng et al., 2017). The *nod* genes code for proteins involved in the synthesis (*nodBCHASUQ*) and exportation (*nodIJ*) of nodulation (Nod) factors, as well as their regulation (*nodD*). In turn, the *nif* genes encode proteins related to the nitrogenase complex (*nifH*, *nifD*, and *nifK*), regulation (*nifA*), and maturation processes (*nifEDXQ*). The *fix* genes encode membrane proteins required for electron transfer to generate the energy required for the SNF process (*fixABCX*; *fixNOPQ*).

54  
55  
56  
57  
58  
59  
60  
61  
62  
63  
64  
65

In beta-rhizobia, *nod* genes are induced in the presence of pure flavonoids such as luteolin and apigenin (Marchetti et al., 2011; Rodríguez-Esperón et al., 2022) or root exudates of the host plant *Mimosa pudica* (Klonowska et al., 2018). In line with the conservation of this important recognition mechanism, other genes and molecules involved in bacteria-plant interaction have been identified in beta-rhizobia. These include the type-III secretion system (Saad et al., 2012) and synthesis of branched-chain amino acids in *Cupriavidus taiwanensis* LMG19424 (Chen et al., 2012); type VI secretion system (de Campos et al., 2017; Lardi et al., 2017) and synthesis of exopolysaccharide (EPS) cepacian in *Paraburkholderia phymatum* STM815 (Liu et al., 2020). Despite these few examples, there is still a lack of knowledge about the molecular mechanisms implicated in the symbiotic interaction between beta-rhizobia and legume hosts.

56  
57  
58  
59  
60  
61  
62  
63  
64  
65

In Uruguay, beta-rhizobia have been identified as the main symbionts of *Parapiptadenia rigida* (Taulé et al., 2012) and *Mimosa* spp. (Platero et al., 2016;

1  
2  
3  
4  
5  
6  
7  
8  
9  
10  
11  
12  
13  
14  
15  
16  
17  
18  
19  
20  
21  
22  
23  
24  
25  
26  
27  
28  
29  
30  
31  
32  
33  
34  
35  
36  
37  
38  
39  
40  
41  
42  
43  
44  
45  
46  
47  
48  
49  
50  
51  
52  
53  
54  
55  
56  
57  
58  
59  
60  
61  
62  
63  
64  
65

68 Pereira-Gómez et al., 2020). Phylogenetic analyses indicated that *Cupriavidus*  
69 strains symbiotically associated with these plants do not belong to the well-  
70 studied *C. taiwanensis* species but rather to the *C. necator* and other *Cupriavidus*  
71 species.

72 *Cupriavidus* sp. UYMMa02A was isolated from nodules of *Mimosa magentea*, a  
73 native legume found in the southeast region of Uruguay. Through a Multi-Locus  
74 Sequence Analysis (MLSA) approach, it was demonstrated that UYMMa02A  
75 does not belong to the previously described *C. taiwanensis* and *C. necator*, but it  
76 may represent a novel rhizobial species within the *Cupriavidus* genus (Platero et  
77 al., 2016). Genome sequencing of *Cupriavidus* sp. UYMMa02A (Iriarte et al.,  
78 2016) indicated the presence of a conserved and compact symbiotic island that  
79 encodes for the *nod*, *nif*, and *fix* genes observed in other beta-rhizobia (Amadou  
80 et al., 2008; Moulin et al., 2014; Sofie E De Meyer et al., 2015, 2016; Sofie E. De  
81 Meyer et al., 2015). In addition, this strain induces pink nodules on the roots of  
82 its original host and other *Mimosa* species, including *M. pudica* (Platero et al.  
83 2016).

84 The present study aimed to analyze the initial steps of the *Cupriavidus-Mimosa*  
85 symbiotic interaction. Firstly, we determined the expression of *nod* genes in  
86 *Cupriavidus* sp. UYMMa02A strain when cultivated in the presence of pure  
87 flavonoids or *Mimosa spp.* root exudates. Then we analyzed the proteomic  
88 changes induced in the bacteria by the presence of pure flavonoids and the plant  
89 host. Finally, we integrated the obtained results into a model that reports the  
90 changes occurring during the initial steps of the *Cupriavidus* sp. UYMMa02A -  
91 *Mimosa pudica* symbiotic interaction.

1  
2  
3  
4  
5  
6  
7  
8  
9  
10  
11  
12  
13  
14  
15  
16  
17  
18  
19  
20  
21  
22  
23  
24  
25  
26  
27  
28  
29  
30  
31  
32  
33  
34  
35  
36  
37  
38  
39  
40  
41  
42  
43  
44  
45  
46  
47  
48  
49  
50  
51  
52  
53  
54  
55  
56  
57  
58  
59  
60  
61  
62  
63  
64  
65

## 92 **Material and Methods**

93 **Bacterial strains, plasmids, and growth conditions.** The bacteria and  
94 plasmids used in this study are listed in Table 1. *Escherichia coli* strains were  
95 grown aerobically at 37°C in Luria–Bertani (LB) medium. *Cupriavidus* strains  
96 were grown at 30°C in LB or M9 minimal medium containing 14mM sodium citrate  
97 as a carbon source (Sambrook et al., 1989). When indicated M9 cultures were  
98 supplemented with 5 µM luteolin or apigenin. Modified M9 media containing  
99 *Mimosa spp.* root exudates were prepared to replace the original water volume  
100 used in M9, by filter-sterilized root exudates. When required the following  
101 antibiotics were used for strain selection; Ampicillin 100 µg.ml<sup>-1</sup> (Ap),  
102 Nitrofurantoin 50 µg.ml<sup>-1</sup> (Nf), Chloramphenicol 25 µg.ml<sup>-1</sup> (Cf), and Tetracycline  
103 8 µg.ml<sup>-1</sup> (Tc).

104 **Sequence Analysis.** Homology searches and sequences retrieval were done via  
105 Internet server BLAST (NCBI, NIH, Bethesda, MD, USA: <http://www.ncbi.nlm.nih.gov>)  
106 and RAST server (Aziz et al., 2008). Sequence alignments were done by  
107 Mega v7.0.26 (Kumar et al., 2016) and SnapGene® software (from Insightful  
108 Science; available at [snapgene.com](http://snapgene.com)) was used for graphic presentation.

109 **Reporter strains construction.** To evaluate the expression of *nodB* gene  
110 promoter, plasmid pCBM01 containing the *pnodB*<sub>19424</sub>-*lacZ* transcriptional fusion  
111 (Marchetti et al., 2010) or plasmid pCZ388 containing a promoterless *lacZ*  
112 (Cunnac et al., 2004) were introduced in *Cupriavidus spp.* strains by triparental  
113 mating as previously described (Rodríguez-Esperón et al., 2022).

1  
2  
3  
4  
5  
6  
7  
8  
9  
10  
11  
12  
13  
14  
15  
16  
17  
18  
19  
20  
21  
22  
23  
24  
25  
26  
27  
28  
29  
30  
31  
32  
33  
34  
35  
36  
37  
38  
39  
40  
41  
42  
43  
44  
45  
46  
47  
48  
49  
50  
51  
52  
53  
54  
55  
56  
57  
58  
59  
60  
61  
62  
63  
64  
65

114 **Assessment of *pnodB*<sub>19424</sub>-*lacZ* gene expression.** Cultures of *Cupriavidus*  
115 *spp.* strains carrying the plasmids pCBM01 or pCZ388 were grown overnight at  
116 30°C using a rotary shaker at 200 rpm, in 5 mL of M9 supplemented with Tc. At  
117 the end of this time, a 1/100 (v/v) dilution was made in fresh medium  
118 supplemented with 5 µM luteolin (≥98% TLC, SIGMA, USA) or in a modified M9  
119 prepared with roots exudates and incubated for 18 h at 30°C. Uninduced control  
120 cultures were included for each assay. Beta-galactosidase assays were  
121 performed according to the standard Miller assay (Miller, 1972).

122 **Pre-treatment, surface sterilization, and germination of *Mimosa spp.* seeds.**

123 *M. pudica* seeds were obtained commercially from Outsidepride Seeds, LLC  
124 (Oregon, USA). *M. magentea* seeds were collected from native plant populations  
125 growing in Uruguay (Platero et al., 2016). The seeds were submerged in ethanol  
126 95% for 2 min and dried in filter paper. After they were treated with 10 M sulfuric  
127 acid for 20 min, followed by seven washes with sterile distilled water. Finally, the  
128 seeds were treated with 4% sodium hypochlorite for 5 min followed by seven  
129 washes with sterile distilled water. Surface-sterilized seeds were germinated on  
130 0.8% (wt/vol) agar-water plates, at 30°C in dark conditions for 2 days.

131 **Roots exudate collection method.** *Mimosa spp.* pre-germinated seeds were  
132 sown in a 250 ml test glass jar (20 seeds per flask) containing 20 ml of sterile  
133 water and a stainless-steel grate for seedling support. Plants were incubated for  
134 five days under a photoperiod of 16h light/8h darkness at 26°C. After that, the  
135 water solution containing the roots exudates was collected in 50 mL plastic  
136 conical tubes, centrifuged for 5 min at 6,000 g to remove cellular debris and  
137 supernatants were filtered-sterilized using 0.45 µm membrane filters (Millipore,



1  
2  
3  
4  
5  
6  
7  
8  
9  
10  
11  
12  
13  
14  
15  
16  
17  
18  
19  
20  
21  
22  
23  
24  
25  
26  
27  
28  
29  
30  
31  
32  
33  
34  
35  
36  
37  
38  
39  
40  
41  
42  
43  
44  
45  
46  
47  
48  
49  
50  
51  
52  
53  
54  
55  
56  
57  
58  
59  
60  
61  
62  
63  
64  
65

138 USA). Filter-sterilized root exudates were used, instead of water, for preparing  
139 modified M9 media. All experiments including root exudates were performed with  
140 freshly (same day) prepared root exudates

141 **Gene expression based on quantitative reverse transcription-PCR (RT-**  
142 **qPCR).** The RT-qPCR experiments were performed with *Cupriavidus sp.*  
143 UYMMa02A growing in M9 with *M. pudica* root exudates or M9 media. For the  
144 bacterial RNA extraction, *Cupriavidus sp.* UYMMa02A was cultivated in 150 mL  
145 of modified M9 with *M. pudica* root exudates or M9 until reaching the mid-  
146 exponential phase (OD<sub>600</sub> between 0.6 - 0.8). Cultures were then incubated for  
147 20 min with 100 µg/ml chloramphenicol and then rapidly cooled by placing the  
148 tubes in a water-ice bath. Cells were recovered by centrifuging at 5000 g for 5  
149 min at 4°C. Obtained pellets were suspended in 1.5 mL of lysis buffer (20 mM  
150 Tris-HCl Buffer pH 7.6; 50 mM MgCl<sub>2</sub>; 150 mM NH<sub>4</sub>Cl and transferred to 2 mL  
151 lysis tubes (MP Biomedicals Lysing Matrix Tubes # Matrix B). Cell lysis was  
152 carried out on Fast Prep equipment (MP Biomedicals) using a cycle of 6.0 m/s  
153 for 60 seconds. Finally, lysates were centrifuged at 10,000 g for 20 min at 4°C,  
154 and supernatants containing the cell extract were transferred to a new tube. One  
155 hundred microliters of the obtained extracts were used for total RNA extraction  
156 using a PureLink RNA Mini Kit (Thermo Fisher Scientific #12183018A). Obtained  
157 RNA was treated with 5 units of DNase I (Thermo Fisher Scientific EN0521) for  
158 5 minutes at 37°C. One microgram of total RNA was converted to cDNA using  
159 the High-Capacity cDNA Reverse Transcription Kit (Applied Biosystem), following  
160 the manufacturer's recommendations. Quantitative PCR (qPCR) analyses were  
161 performed essentially as described (Rodríguez-Esperón et al., 2022). The  
162 UYMMa02A *efg* gene (ODV42482.1) which encodes for the elongation factor G

1  
2  
3  
4  
5  
6  
7  
8  
9  
10  
11  
12  
13  
14  
15  
16  
17  
18  
19  
20  
21  
22  
23  
24  
25  
26  
27  
28  
29  
30  
31  
32  
33  
34  
35  
36  
37  
38  
39  
40  
41  
42  
43  
44  
45  
46  
47  
48  
49  
50  
51  
52  
53  
54  
55  
56  
57  
58  
59  
60  
61  
62  
63  
64  
65

163 and the *s14* gene (ODV43065.1) which encodes for the ribosome protein S14,  
164 were used as reference genes. The UYMMa02A *nodA*, *nodB*, and *nodC* genes  
165 were selected to analyze relative gene expression. Primer Blast software was  
166 used to design primer sets for *nodA*, *nodB*, *nodC*, *efg*, and *s14*. The following  
167 primers were used: *efg*-for (5'-GCGATCATTGGGACGAAGC-3'); *efg*-rev (5'-  
168 CGGACTCGACCATCTTCTCG-3'); *s14*-for (5'-CTGTTCTACGTGTCAG-3');  
169 *s14*-rev (5'-TGATGTTGATGCGGTGTTTC-3'); *nodA*-for (5'-  
170 ACGTCCTCGCTGTGATTCTG-3'); *nodA*-rev (5'-  
171 AGGTCCGTTGCGTTGATAG-3'); *nodB*-for (5'-  
172 TGGGGCAATTCAGCTTCCA-3'); *nodB*-rev (5'-  
173 AGCGACTTCGTGTCCTTCAG-3'); *nodC*-for (5'-  
174 CAGAGCTTGCCTCACTTCCA-3'); *nodC*-rev (5'-  
175 TGCATCGTCCTCATAGTCGC-3'). qPCRs were performed on a C1000 Touch  
176 Thermal Cycler (Bio-Rad) using the iQTM SYBR Green Supermix (Bio-Rad).  
177 qPCRs conditions were as follows: 5 min at 95°C, 40 cycles of 15 s at 95°C, 30 s  
178 at 60°C and 30 s at 72°C. Primer specificity and dimer formation were checked  
179 by dissociation curves. A mixture of cDNA from induced and non-induced  
180 samples was used for calculating primer efficiency. The relative gene expression  
181 level was calculated using the  $2^{-\Delta\Delta Cq}$  method, statistical analyses were performed  
182 in the InfoStat statistical program (<https://www.infostat.com.ar/>). Normal  
183 distribution of data was confirmed using the Shapiro-Wilk test and one-way  
184 ANOVA was used for sample comparisons. Differences were considered  
185 statistically significant if the p-value <0.05.

186 **Assessment of growth promotion capacity.** Germinated seeds prepared as  
187 described above were transferred into glass tubes containing 15 mL of Jensen's

1  
2  
3  
4  
5  
6  
7  
8  
9  
10  
11  
12  
13  
14  
15  
16  
17  
18  
19  
20  
21  
22  
23  
24  
25  
26  
27  
28  
29  
30  
31  
32  
33  
34  
35  
36  
37  
38  
39  
40  
41  
42  
43  
44  
45  
46  
47  
48  
49  
50  
51  
52  
53  
54  
55  
56  
57  
58  
59  
60  
61  
62  
63  
64  
65

188 N-free medium (36) solidified with 0.8% (wt/vol) agar. Seedlings were inoculated  
189 with 1 mL of a rhizobial suspension containing  $1 \times 10^7$  cfu. One milliliter of sterile  
190 water was added to negative controls. Plants were grown under a photoperiod of  
191 16h light/8h darkness at 26°C. The presence and coloration of root nodules were  
192 evaluated periodically. Three months after inoculation, plants were harvested,  
193 and plant height was measured and used as a proxy for the plant growth  
194 promotion capacity of inoculated strains. The experiment was repeated three  
195 times with at least 10 plants per condition. Differences were considered  
196 statistically different if the p-value < 0.01 according to the t-test.

197 ***Cupriavidus sp. UYMMa02A-Mimosa pudica* co-culture assays.** A co-culture  
198 device was constructed allowing bacterial-plant signal exchange, but avoiding  
199 physical contact between both organisms (Fig. 8). Bacterial containers were  
200 assembled using 10 cm dialysis membrane tubing pieces (D9652, Sigma  
201 Aldrich). Membranes were washed with distillate water and one of their ends was  
202 sealed with a double knot, the other end was attached to a 10 cm silicone tubing  
203 and sealed with a plastic seal. For a complete and tight seal, a small glass tube  
204 was inserted inside the silicone tubing. Bacterial container sterilization was  
205 achieved by gamma-irradiation using a 21 kGy dose in the irradiation facilities of  
206 the Uruguayan Technological Laboratory (LATU). Test glass jars of 250 mL  
207 containing 50 mL of N-free Howieson (Howieson et al., 1993) liquid media diluted  
208 1/10 (v/v) and polypropylene balls as seedling support, were autoclaved for 20  
209 minutes at 121°C. After cooling, the jars were opened in the laminar flow hoods,  
210 and bacterial containers were aseptically added, submerging the membrane in  
211 the media and the silicone tubing facing the jar lids. A total of 50 *M. pudica*  
212 germinated seeds were sown in each jar and incubated under a photoperiod of

1  
2  
3  
4  
5  
6  
7  
8  
9  
10  
11  
12  
13  
14  
15  
16  
17  
18  
19  
20  
21  
22  
23  
24  
25  
26  
27  
28  
29  
30  
31  
32  
33  
34  
35  
36  
37  
38  
39  
40  
41  
42  
43  
44  
45  
46  
47  
48  
49  
50  
51  
52  
53  
54  
55  
56  
57  
58  
59  
60  
61  
62  
63  
64  
65

213 16h light/8h darkness. After 5 days, the bacterial containers were filled through  
214 the silicone tubing, with 5 mL of  $1 \times 10^8$  cfu.mL<sup>-1</sup> of *Cupriavidus* sp. UYMMa02A,  
215 and incubated for another five days under the same conditions of temperature  
216 and photoperiod. As control treatments, plant-free systems were used. In these  
217 cases, Howieson liquid media was supplemented with 2 mM sodium citrate as a  
218 carbon source and 2 mM ammonium chloride as a nitrogen source, to allow  
219 bacterial survival. Cell suspensions were carefully transferred from the  
220 membranes to clean and sterile plastic tubes and centrifuged for 5 min at 6,000  
221 g. Bacterial pellets were used for total protein extraction. A minimum of three  
222 biological replicates were performed for each sample.

223 **Total protein extraction and solubilization.** For protein extraction, bacterial  
224 pellets were washed three times with 2 mL of phosphate-buffered saline (PBS)  
225 and resuspended in 10% of the original culture volume in PBS containing 1X  
226 complete-EDTA-Free protease inhibitor (Roche). Cell lysis was performed by  
227 sonication (7 cycles x 30 sec) in continuous mode and at a relative power of 4  
228 alternated with 30 sec of rest in an ice-water bath, using an ultrasonic  
229 homogenizer (Cole-Parmer Instruments Co.). Cell lysates were separated by  
230 centrifugation at 12,000 g for 15 min at 4°C and the supernatant containing the  
231 total soluble proteins was kept at -20°C. At least three biological replicates were  
232 performed per sample.

233 **Protein quantification.** Protein concentration was estimated by the Bradford  
234 method (Bradford, 1976) using bovine serum albumin (BSA) for calibration  
235 curves. The quality of protein fractions was verified by SDS-PAGE (Laemmli,  
236 1970).

1  
2  
3  
4  
5  
6  
7  
8  
9  
10  
11  
12  
13  
14  
15  
16  
17  
18  
19  
20  
21  
22  
23  
24  
25  
26  
27  
28  
29  
30  
31  
32  
33  
34  
35  
36  
37  
38  
39  
40  
41  
42  
43  
44  
45  
46  
47  
48  
49  
50  
51  
52  
53  
54  
55  
56  
57  
58  
59  
60  
61  
62  
63  
64  
65

237 **Protein precipitation.** Previous to two-dimensional (2D) electrophoresis,  
238 proteins were precipitated, washed, and concentrated, using the commercial kit  
239 “2-D Clean Up Kit” (GE Healthcare, Amersham Biosciences) according to the  
240 manufacturer's instructions. Finally, proteins were resuspended in a rehydration  
241 buffer (8M urea, 2M thiourea, 4% CHAPS, 40mM DTT, 1.2% (v/v) IPG buffer) pH  
242 8.5.

243 **Protein labelling.** Thirty-five µg of total proteins from each condition were  
244 labeled using the Refraction-2D™ Labelling Kit (NH DyeAGNOSTICS GmbH,  
245 Germany), following the manufacturer's recommendations. The samples were  
246 normalized and labeled with the Cy3 dye ( $\lambda_{\text{exc}} = 532\text{nm}$ / $\lambda_{\text{em}} = 580\text{nm}$ ) or Cy5  
247 ( $\lambda_{\text{exc}} = 633\text{nm}$ / $\lambda_{\text{em}} = 670\text{nm}$ ), while Cy2 dye ( $\lambda_{\text{exc}} = 488\text{nm}$ / $\lambda_{\text{em}} = 520\text{nm}$ ) was  
248 used to label the internal standard which consists of a pooled sample comprising  
249 equal amounts (10 µg) of all samples to be compared.

250  
251 **2D-DIGE Electrophoresis.** The labeled samples were mixed in hydration buffer  
252 (8M urea, 2M thiourea, 2% (p/v) CHAPS, and 1.2% (v/v) IPG-buffer) and loaded  
253 on 24-cm Immobiline DryStrips previously hydrated in the same buffer (nonlinear  
254 pH range 3–10, GE Healthcare). Isoelectric focusing (IEF) was run using an  
255 IPGphor III apparatus (GE Healthcare). The voltage profile used was adapted to  
256 run overnight with the following voltage program: constant phase of 500V/2h,  
257 constant phase of 2000V/2h, a linear increase to 4000V/2h, a linear increase to  
258 8000V/2h, and a constant final phase at 8000V for 4h. After that, the IPG strips  
259 were allowed to equilibrate for 10 minutes with mechanical agitation in 1mL of  
260 equilibration buffer (6 M urea, 50 mM Tris–HCl, pH 8.6, 30% glycerol, 2 % sodium  
261 dodecyl sulfate) containing 1 % DDT for 10 min. Then, reactions were quenched

1  
2  
3  
4  
5  
6  
7  
8  
9  
10  
11  
12  
13  
14  
15  
16  
17  
18  
19  
20  
21  
22  
23  
24  
25  
26  
27  
28  
29  
30  
31  
32  
33  
34  
35  
36  
37  
38  
39  
40  
41  
42  
43  
44  
45  
46  
47  
48  
49  
50  
51  
52  
53  
54  
55  
56  
57  
58  
59  
60  
61  
62  
63  
64  
65

262 by immersing the strips in SDS-PAGE running buffer (25 mM Tris, 192 mM  
263 glycine, 0.1% SDS). As a second dimension, proteins were separated by SDS-  
264 PAGE gels (12% acrylamide-bisacrylamide) using an Ettan DALT-Six apparatus  
265 Electrophoresis System electrophoresis cell maintained at 20°C with the  
266 Multitemp III cooling unit (GE Healthcare). Each strip was placed on the  
267 corresponding acrylamide gel and bound to it, using a running buffer containing  
268 0.2 % agarose and 0.002% (w/v) bromophenol blue. The runs were carried out  
269 at 100 mA and 80 V for the first 5 min and then the voltage was increased to 120  
270 V until the run front reached the end of the gel.

271

272 **Image Analysis.** After 2D-DIGE electrophoresis, gels were fixed with ethanol:  
273 acetic acid: H<sub>2</sub>O (5:1:4) solution for 30 min. They were then scanned using a  
274 Typhoon 9500 FLA scanner (GE Healthcare), using the parameters  
275 recommended by the manufacturer, and analyzed using ImageQuant TL v8.1  
276 software (GE Healthcare). The SameSpots software (TotalLab, Newcastle, UK)  
277 was used to match and analyze protein spots, allowing the detection,  
278 normalization with the internal standard, and quantification of the spots.  
279 Differential-in-gel analysis was used to calculate protein abundance alterations  
280 between samples on the same gel. The resulting spot maps for each biological  
281 replicate were then analyzed through biological variation analysis to provide  
282 statistical data on the differential protein expression. Spots that exhibited  
283 differences in the level of fluorescence with a p-value  $\leq 0.05$  and a rate of change  
284  $\geq 1.25$  were considered as differentially regulated and selected for identification.

285

286 **Spot picking, protein digestion, and MALDI-TOF/TOF protein identification.**

287 To identify the differentially expressed proteins, gels were stained using  
288 Coomassie Brilliant Blue G-250 (Bio-Rad, Hercules, CA). Spots presenting  
289 significant differences were excised from gels, unstained with a solution of 0.1M  
290  $\text{NH}_4\text{HCO}_3$  in acetonitrile (ACN) 50% (v/v) and in-gel digested overnight using  
291 modified sequencing grade trypsin (Promega, Madison, USA). Peptide extraction  
292 was performed as previously described (Gil et al., 2019) and samples were  
293 desalted using Zip-Tip C18 reverse phase microcolumns (Millipore, Merck, USA)  
294 eluted directly on the plate using matrix solution ( $\alpha$ -cyano-4-hydroxycinnamic acid  
295 in 60 % ACN, 0.1 % TFA). The mixture was spotted onto an Opti-TOF plate of  
296 384 positions (Ab Sciex). Spectra acquisition was performed on a MALDI-  
297 TOF/TOF MS (4800 Analyzer Abi Sciex) operated in positive reflector mode. The  
298 collected MS and MS/MS spectra of selected ions were externally calibrated  
299 using a standard peptide mix (Applied Biosystems). Protein identification was  
300 carried out using Mascot (Matrix Science, London, UK,  
301 (<http://www.matrixscience.com>) in Sequence query mode, using the genome of  
302 *Cupriavidus* sp. UYMMa02A (GCA\_001725945.1) or the NCBI NR databases.  
303 The search parameters were: Unrestricted taxonomy; allowable trypsin cleavage  
304 jumps = 1; partial modifications: oxidation of methionine and alkylation of cysteine  
305 by carbamidomethylation; peptide mass tolerance = 0.05Da and MS/MS  
306 tolerance = 0.45Da. For protein identification at least one MS/MS spectra per  
307 protein was required (with a Mascot peptide ion score  $p < 0.05$ ) and a p-value  
308  $p < 0.05$  in the Mascot protein score. Proteins were classified into COGs functional  
309 categories and assigned to KEGG pathways using eggNOG-mapper (Huerta-  
310 Cepas et al., 2016) and also classified according to their subcellular location with

1  
2  
3  
4  
5  
6  
7  
8  
9  
10  
11  
12  
13  
14  
15  
16  
17  
18  
19  
20  
21  
22  
23  
24  
25  
26  
27  
28  
29  
30  
31  
32  
33  
34  
35  
36  
37  
38  
39  
40  
41  
42  
43  
44  
45  
46  
47  
48  
49  
50  
51  
52  
53  
54  
55  
56  
57  
58  
59  
60  
61  
62  
63  
64  
65

311 the CELLO v.2.5 (Cheng et al., 2014). The genomic context of the proteins and  
312 the location of their gene sequence at the chromosomal level were analyzed by  
313 blast searches against the *Cupriavidus* sp. UYMMa02A genome annotated in the  
314 RAST server (Aziz et al., 2008).  
315



1  
2  
3  
4  
5  
6  
7  
8  
9  
10  
11  
12  
13  
14  
15  
16  
17  
18  
19  
20  
21  
22  
23  
24  
25  
26  
27  
28  
29  
30  
31  
32  
33  
34  
35  
36  
37  
38  
39  
40  
41  
42  
43  
44  
45  
46  
47  
48  
49  
50  
51  
52  
53  
54  
55  
56  
57  
58  
59  
60  
61  
62  
63  
64  
65

## 316 Results

317

318 *The genome of Cupriavidus sp. UYMMa02A encodes a highly conserved*  
319 *symbiotic island.*

320 The draft genome of *Cupriavidus sp. UYMMa02A* was published in 2016 (Iriarte  
321 et al., 2016). Genome comparison among beta-rhizobial strains revealed a high  
322 level of synteny and nucleotide identity in operons containing the *nod*, *nif*, and *fix*  
323 genes (Fig. 1). However, there were differences in non-symbiotic and  
324 transposon-related genes within the symbiotic islands leading to length  
325 heterogeneity among them. The symbiotic island of *Cupriavidus sp. UYMMa02A*  
326 was the shortest with a predicted length of 33,908 bp.

327 A closer inspection of the *nod* operon in *Cupriavidus sp. UYMMa02A* indicated  
328 that eight *nod* genes, involved in Nod factors biosynthesis and exportation,  
329 namely *nodBCIJAHSUQ*, are arranged in a single operon, while the *nodD* gene  
330 encoding a LysR-type transcriptional regulator, was located in the opposite  
331 orientation of *nodB* gene (Fig. 2). Moreover, a conserved NodD DNA binding  
332 motif known as nod-box (Schlaman et al., 1992) was identified in the intergenic  
333 region between *nodD* and *nodB* genes (Fig. 2). Minor differences in length and  
334 sequence were observed among the compared sequences, with the symbiotic  
335 islands of *Cupriavidus sp. UYMMa02A* and *Cupriavidus necator* UYPR2.512,  
336 showing the highest sequence homology.

337 The *UYMMa02A nod* operon is not induced by pure flavonoids.

1  
2  
3  
4  
5  
6  
7  
8  
9  
10  
11  
12  
13  
14  
15  
16  
17  
18  
19  
20  
21  
22  
23  
24  
25  
26  
27  
28  
29  
30  
31  
32  
33  
34  
35  
36  
37  
38  
39  
40  
41  
42  
43  
44  
45  
46  
47  
48  
49  
50  
51  
52  
53  
54  
55  
56  
57  
58  
59  
60  
61  
62  
63  
64  
65

338 The flavonoids luteolin and apigenin are known to induce the expression of *nod*  
339 genes in rhizobial *Cupriavidus sp.* strains (Amadou et al., 2008; Marchetti et al.,  
340 2010; Rodríguez-Esperón et al., 2022). **The observed** syntenies lead us to  
341 hypothesize that **the *nod* genes of *Cupriavidus sp.* UYMMa02A** would be  
342 regulated by the same mechanism. To analyze this, *Cupriavidus sp.* UYMMa02A  
343 was transformed with the pCBM01 plasmid containing a *pnodB<sub>19424</sub>-lacZ*  
344 transcriptional fusion and beta-galactosidase (B-gal) activity was compared with  
345 *C. necator* UYPR2.512 and *C. taiwanensis* LMG19424, **both harboring** the same  
346 plasmid. As expected, a strong induction of B-gal activity was observed for *C.*  
347 *necator* UYPR2.512 and *C. taiwanensis* LMG19424 in the presence of luteolin.  
348 However, *Cupriavidus sp.* UYMMa02A **remained** unresponsive to the presence  
349 of pure flavonoids (Fig. 3).

350 *Cupriavidus sp.* UYMMa02A *nod* genes are not induced in the presence of  
351 *Mimosa spp.* root exudates.

352 Considering that *nod* genes expression is regulated by different compounds in  
353 different rhizobial strains (Hungria et al., 1991; Schmidt et al., 1994; Jiménez-  
354 Guerrero et al., 2018), we decided to **investigate whether *Mimosa pudica* and**  
355 ***Mimosa magentea* root exudates could serve as potential inducers** for *nod* genes  
356 **expression** in *Cupriavidus sp.* UYMMa02A. Root exudates are complex solutions  
357 containing different amino acids, organic acids, sugars, and phenolic compounds,  
358 **which have been shown** to induce *nod* gene expression in *C. taiwanensis*  
359 LMG19424 (Klonowska et al., 2018).

360 A clear induction of *nod* gene expression was observed, as indicated by an  
361 increase in B-gal activity when *C. taiwanensis* LMG19424 and ***C. necator***  
362 **UYPR2.512** were grown in the presence of *Mimosa spp.* root exudates (Figs. 4

1  
2  
3  
4  
5  
6  
7  
8  
9  
10  
11  
12  
13  
14  
15  
16  
17  
18  
19  
20  
21  
22  
23  
24  
25  
26  
27  
28  
29  
30  
31  
32  
33  
34  
35  
36  
37  
38  
39  
40  
41  
42  
43  
44  
45  
46  
47  
48  
49  
50  
51  
52  
53  
54  
55  
56  
57  
58  
59  
60  
61  
62  
63  
64  
65

363 and 5). These results indicate that *Mimosa pudica* and *Mimosa magentea* root  
364 exudates contain inducers for *nod* gene expression. However, when *Cupriavidus*  
365 *sp.* UYMMa02A was exposed to these root exudates, we did not observe any  
366 change in B-gal activity, suggesting that *nod* genes expression was not induced  
367 in this strain (Fig. 4 and 5). Similar results were observed when pure flavonoids  
368 were used.

369 Altogether these findings suggest that the *pnodB*<sub>19424</sub>-*lacZ* is not responsive in  
370 *Cupriavidus sp.* UYMMa02A. However, we cannot exclude the possibility that  
371 endogenous *nod* genes in *Cupriavidus sp.* UYMMa02A *nod* genes could be  
372 induced but were not detected by the assay used. To directly assess this, we  
373 analyzed the mRNA levels of *nodA*, *nodB*, and *nodC* in *Cupriavidus sp.*  
374 UYMMa02A in the presence or absence of *M. pudica* root exudates (Fig. 6). No  
375 changes in the relative *nod* gene expression were observed when *Cupriavidus*  
376 *sp.* UYMMa02A was grown in the presence of *M. pudica* root exudates compared  
377 to growth in M9 minimal media. These results confirm the absence of *nod* genes  
378 induction in *Cupriavidus sp.* UYMMa02A.

379  
380 *Cupriavidus sp.* UYMMa02A induces functional nodules and promotes *M. pudica*  
381 *plant growth in Nitrogen-limiting conditions.*

382 We have previously shown that *Cupriavidus sp.* UYMMa02A can form nodules in  
383 the roots of several *Mimosa sp.* including *M. pudica* plants (Platero et al., 2016).  
384 However, there was no direct evidence of this symbiotic interaction's plant growth  
385 promotion ability. When *M. pudica* plants growing in nitrogen-free media were  
386 inoculated with *Cupriavidus sp.* UYMMa02A, we observed the formation of

1  
2  
3  
4  
5  
6 387 reddish nodules in the roots and a significant increase in plant height (Fig. 7),  
7  
8 388 strongly supporting the proficiency of this symbiotic pair.

9  
10  
11 389 *Proteomic changes induced by luteolin and apigenin in Cupriavidus sp.*  
12  
13 390 *UYMMa02A*

14  
15 391 The lack of induction of *nod* genes suggests that alternative mechanisms could  
16  
17 392 be involved in the establishment of the *Cupriavidus sp. UYMMa02A-M. pudica*  
18  
19 393 symbiotic interaction. To determine the significance of this finding, we decided to  
20  
21 394 employ a proteomic approach known as Differential In Gel Expression (DIGE)  
22  
23 395 (Meleady, 2018; Mozejko-Ciesielska and Mostek, 2019). In the first approach,  
24  
25 396 bacteria were grown in the presence of luteolin or apigenin, and total protein  
26  
27 397 profiles were compared with bacteria growing in the absence of the flavonoids.  
28  
29 398 Two-dimensional electrophoresis allowed us to separate 373 different spots,  
30  
31 399 representing around 4.5 % of the CDS encoded by *Cupriavidus sp. UYMMa02A*  
32  
33 400 genome (Iriarte et al., 2016). DIGE analysis showed 17 spots with altered  
34  
35 401 expression levels in the presence of luteolin while 16 spots were differentially  
36  
37 402 expressed in the presence of apigenin. When we performed a combined analysis  
38  
39 403 of differentially expressed spots in the presence of the flavonoids versus the  
40  
41 404 control condition, a total of 22 differentially expressed spots were detected, 8  
42  
43 405 overrepresented in the luteolin condition, 8 in the apigenin condition, and 6 in the  
44  
45 406 control condition. After Coomassie blue staining and gel excision, a total of 9  
46  
47 407 proteins were identified by MALDI-TOF analyses (Table 2). According to COG  
48  
49 408 analyses, 3 of the identified proteins belong to Category E (Amino acid transport  
50  
51 409 and metabolism) and 3 to category C (Energy conversion and production), one  
52  
53 410 protein to Category I (Lipids transport and metabolism), and one belong to  
54  
55 411 category P (inorganic ion transport). Except for the tricarboxylate transporter  
56  
57  
58  
59  
60  
61  
62  
63  
64  
65

1  
2  
3  
4  
5  
6  
7  
8  
9  
10  
11  
12  
13  
14  
15  
16  
17  
18  
19  
20  
21  
22  
23  
24  
25  
26  
27  
28  
29  
30  
31  
32  
33  
34  
35  
36  
37  
38  
39  
40  
41  
42  
43  
44  
45  
46  
47  
48  
49  
50  
51  
52  
53  
54  
55  
56  
57  
58  
59  
60  
61  
62  
63  
64  
65

412 protein TctC with a periplasmic localization, all the identified proteins were  
413 predicted to be cytoplasmic. A model summarizing the major findings using this  
414 approach is shown in Figure 9.

415 *Differential protein expression during Cupriavidus sp. UYMMa02A-Mimosa*  
416 *pudica co-cultures.*

417 The next step in elucidating the mechanisms involved in the plant-bacteria  
418 interaction was to determine the proteomic responses of *Cupriavidus sp.*  
419 UYMMa02A to the presence of plant host *Mimosa pudica*. We implemented a co-  
420 culture device intended to allow plant-bacteria signal interchange, preventing  
421 physical contact between symbionts. In this device, plants were grown  
422 hydroponically with bacteria placed in a closed dialysis membrane submerged in  
423 the same hydroponic solution (Fig. 8). Protein profile expression under co-culture  
424 conditions was compared with bacterial cells cultivated in the same conditions,  
425 but in that case, *Mimosa* plants were not included. The hydroponic solution was  
426 supplemented with minimal amounts of carbon and nitrogen sources to allow  
427 bacterial survival. Image analyses of the 2D gels captured a total of 674 spots,  
428 representing around 8 % of the bacterial encode capacity. Thirty-seven  
429 differentially expressed spots were determined (26 and 11 spots were  
430 overexpressed and repressed respectively). After staining and excision from the  
431 gels, 17 different proteins were identified by MALDI-TOF, belonging to 11  
432 different COG categories. Notably, proteins categorized in the categories O  
433 (posttranslational modifications and chaperones), G (carbohydrate transport and  
434 metabolism), and M (membrane and cell wall) contains both induced and  
435 repressed proteins, while proteins in category T (transduction signals

1  
2  
3  
4  
5  
6  
7  
8  
9  
10  
11  
12  
13  
14  
15  
16  
17  
18  
19  
20  
21  
22  
23  
24  
25  
26  
27  
28  
29  
30  
31  
32  
33  
34  
35  
36  
37  
38  
39  
40  
41  
42  
43  
44  
45  
46  
47  
48  
49  
50  
51  
52  
53  
54  
55  
56  
57  
58  
59  
60  
61  
62  
63  
64  
65

436 mechanisms) were found overexpressed (Table 3). Subcellular localization  
437 analysis identified 9 cytoplasmic proteins, 3 periplasmic proteins, and 1 outer  
438 membrane protein, while 5 proteins were predicted to be found both at the  
439 bacterial cytoplasm and extracellularly. A model integrating the major findings  
440 using this approach is presented in Figure 10.

## 441 **Discussion**

442 The presence of highly conserved symbiotic islands in the genome of rhizobial  
443 *Cupriavidus* spp. suggest the existence of conserved symbiotic mechanisms  
444 among these strains. Notwithstanding, gene expression analyses have indicated  
445 that pure flavonoids or *Mimosa* spp. root exudates are ineffective in inducing  
446 *Cupriavidus* sp. UYMMa02A *nod* genes transcription. This is intriguing since it  
447 has been shown that the presence of luteolin or apigenin induces the synthesis  
448 and exportation of Nod factors in *C. taiwanensis* LMG19424 (Amadou et al.,  
449 2008). In addition, these flavonoids were shown to induce the expression of the  
450 *pnodB<sub>19424</sub>-lacZ* transcriptional fusion present in pCBM01, in both *C. taiwanensis*  
451 LMG19424 (Marchetti et al., 2010) and *C. necator* UYPR2.512 (Rodríguez-  
452 Esperón et al., 2022). It is well known that the flavonoid effect on *nod* genes  
453 regulation is dependent on the NodD regulatory protein (Schlaman et al., 1992).  
454 Different NodD proteins respond to different flavonoids, being this mechanism  
455 one of the bases of the rhizobium-legume specificity (Masson-Boivin et al., 2009).  
456 Small differences could be observed at *Cupriavidus* sp. UYMMa02A NodD  
457 protein sequence and in the *nodB-nodD* intergenic sequence in comparison with  
458 *C. taiwanensis* LMG19424 and *C. necator* UYPR2.512. Thus, it is possible that  
459 *Cupriavidus* sp. UYMMa02A NodD protein does not become activated by the

1  
2  
3  
4  
5  
6  
7  
8  
9  
10  
11  
12  
13  
14  
15  
16  
17  
18  
19  
20  
21  
22  
23  
24  
25  
26  
27  
28  
29  
30  
31  
32  
33  
34  
35  
36  
37  
38  
39  
40  
41  
42  
43  
44  
45  
46  
47  
48  
49  
50  
51  
52  
53  
54  
55  
56  
57  
58  
59  
60  
61  
62  
63  
64  
65

460 presence of flavonoids or this protein could not recognize the *C. taiwanensis*  
461 LMG19424 *nodB* promoter region present in the *pnodB*<sub>19424</sub>-*lacZ* used here. To  
462 overcome these limitations, we used *M. magentea* and *M. pudica* root exudates  
463 for *nod* genes expression analyses, however no changes in the expression levels  
464 of *nod* genes in *Cupriavidus* sp. UYMMa02A were observed. These results  
465 indicated that in *Cupriavidus* sp. UYMMa02A *nod* genes may not be involved in  
466 the first steps of the symbiotic interaction and suggest the existence of alternative  
467 mechanisms to Nod factors for bacterial-plant interaction. It is now known that  
468 some rhizobial strains are naturally able to engage in symbiotic interactions with  
469 their plant host in a Nod-factor-independent way. Researchers have discovered  
470 strains of *Bradyrhizobium* sp. lacking the canonical *nodABC* genes that can  
471 effectively nodulate *Aeschynomene* spp. (Giraud et al., 2007; Miché et al., 2010)  
472 and *Arachis hypogaea* (Guha et al., 2022).

473 The lack of induction of *nod* genes in *Cupriavidus* sp. UYMMa02A prompted us  
474 to search for alternative mechanisms involved in bacterial-plant interaction. To  
475 identify proteins potentially implicated in the initial steps of this process, we  
476 analyzed the patterns of protein expression of *Cupriavidus* sp. UYMMa02A when  
477 exposed to pure flavonoids and during plant co-culture conditions. The response  
478 to different *nod* gene-inducing flavonoids and root exudates derived from the  
479 plant host has been studied in various rhizobial species, mostly belonging to the  
480 alpha-proteobacteria class, using transcriptomic and proteomic approaches  
481 (Jiménez-Guerrero et al., 2017; diCenzo et al., 2019). These studies have  
482 demonstrated, that in addition to *nod* genes, flavonoids, and root exudates can  
483 influence the expression of several bacterial genes encoded by different bacterial  
484 replicons. When comparing the responses to flavonoids, and root exudates,

1  
2  
3  
4  
5  
6  
7  
8  
9  
10  
11  
12  
13  
14  
15  
16  
17  
18  
19  
20  
21  
22  
23  
24  
25  
26  
27  
28  
29  
30  
31  
32  
33  
34  
35  
36  
37  
38  
39  
40  
41  
42  
43  
44  
45  
46  
47  
48  
49  
50  
51  
52  
53  
54  
55  
56  
57  
58  
59  
60  
61  
62  
63  
64  
65

485 there is only partial overlap, particularly in *nod*-related genes, indicating that  
486 specific mechanisms are regulated in response to distinct stimuli (Capela et al.,  
487 2005). In addition, these responses are often specific to the genus and strains of  
488 rhizobia (Fagorzi et al., 2021).

489 Only two works that used omics approaches have been published for the analysis  
490 of rhizobial *Cupriavidus* strains response to flavonoids (Rodríguez-Esperón et al.,  
491 2022) or host root exudates (Klonowska et al., 2018). Both works showed the  
492 differential expression of hundreds of genes, located at different bacterial  
493 replicons, in response to these stimuli. In agreement with this, upon luteolin and  
494 apigenin or co-culture conditions, *Cupriavidus sp.* UYMMa02A experiences  
495 significant changes at the proteomic level. Approximately 6 % (22 out of 357  
496 spots) of the *Cupriavidus sp.* UYMMa02A proteome changed in response to the  
497 presence of flavonoids, suggesting that these molecules are indeed signal  
498 molecules for this *Cupriavidus sp.* strain. In agreement with the observed lack of  
499 induction of the *pnodB<sub>19424</sub>-lacZ* transcriptional fusion, we did not detect the  
500 differential expression of proteins belonging to the symbiotic Island. Indeed, most  
501 of the affected proteins identified were related to the energy conversion and  
502 production (C) and amino acid metabolism (E) COG categories, indicating that  
503 flavonoids induce metabolic changes in *Cupriavidus sp.* UYMMa02A. The  
504 overexpression of the tricarboxylate transport protein (TctC) could reflect an  
505 increase in citrate transport, the only carbon source in the used media. Under  
506 these conditions, citrate would be incorporated into the *Cupriavidus* metabolism  
507 directly through the citrate cycle (TCA or Krebs cycle), serving as an energy  
508 source and a carbon skeleton source. However, the concomitant diminution of  
509 the E2 component of the 2-oxoglutarate dehydrogenase complex would slow



1  
2  
3  
4  
5  
6  
7  
8  
9  
10  
11  
12  
13  
14  
15  
16  
17  
18  
19  
20  
21  
22  
23  
24  
25  
26  
27  
28  
29  
30  
31  
32  
33  
34  
35  
36  
37  
38  
39  
40  
41  
42  
43  
44  
45  
46  
47  
48  
49  
50  
51  
52  
53  
54  
55  
56  
57  
58  
59  
60  
61  
62  
63  
64  
65

510 down the conversion of 2-oxo-glutarate (2-OG) to Succinyl-CoA. This change  
511 would **result in** the accumulation of 2-OG, a key biosynthetic intermediate **that**  
512 **connects** carbon and nitrogen metabolism. The 2-OG molecule is also involved  
513 in modulating enzyme activity and detoxifying reactive oxygen species (ROS)  
514 (Huergo and Dixon, 2015). Considering this, our result **may indicate** that **some of**  
515 the metabolic changes observed after **exposure to** luteolin and apigenin in  
516 *Cupriavidus sp.* UYMMa02A could be related to an oxidative stress response. In  
517 that sense, Mailloux and collaborators have shown that in response to oxidative  
518 stress, *Pseudomonas fluorescence* increased the activity of an NADP-dependent  
519 isocitrate dehydrogenase while decreasing the activity of the 2-oxoglutarate  
520 dehydrogenase complex, leading to the accumulation of 2-OG (Mailloux et al.,  
521 2007). **Supporting** this hypothesis, we also observed a rise in the DNA  
522 starvation/stationary phase protection protein (DpsA), **which belongs to** the  
523 ferritin superfamily **and is** involved in DNA binding and protection during  
524 starvation and/or oxidative stress conditions (Martinez and Kolter, 1997;  
525 Gambino and Cappitelli, 2016; Orban and Finkel, 2022). Since luteolin and  
526 apigenin **have been reported to** scavenge ROS (Wu et al., 2015; Salehi et al.,  
527 2019; Caporali et al., 2022), it is **unlikely** that the flavonoids **themselves** are  
528 **causing** oxidative stress. Instead, the flavonoids **may act** as signals, advertising  
529 that oxidative **could occur** during the forthcoming interaction with plant roots, as  
530 the local production of ROS is a common feature observed during plant-bacteria  
531 interactions (Oldroyd et al., 2011; Gourion et al., 2015; Janczarek, Rachwał,  
532 Marzec, et al., 2015).

533 The **increased levels** of the bifunctional **enzyme** Aspartate-Transaminase /  
534 Aspartate-4-decarboxylase (AsdA) and the Branched chain amino acids

1  
2  
3  
4  
5  
6  
7  
8  
9  
10  
11  
12  
13  
14  
15  
16  
17  
18  
19  
20  
21  
22  
23  
24  
25  
26  
27  
28  
29  
30  
31  
32  
33  
34  
35  
36  
37  
38  
39  
40  
41  
42  
43  
44  
45  
46  
47  
48  
49  
50  
51  
52  
53  
54  
55  
56  
57  
58  
59  
60  
61  
62  
63  
64  
65

535 aminotransferase (IlvE) in the presence of luteolin and apigenin suggest that  
536 flavonoids impact amino acid metabolism in *Cupriavidus sp.* UYMMa02A. AsdA  
537 catalyzes the transamination of oxaloacetate to L-Aspartate and the subsequent  
538 decarboxylation of aspartate to alanine (Kakimoto et al., 1969; Chen et al., 2000).  
539 The exportation of alanine and aspartate, through an amino acid cycle between  
540 bacteroids and plants, has been postulated to be important for SNF (Prell and  
541 Poole, 2006; Prell et al., 2009). Besides this, the increase in the IlvE  
542 aminotransferase levels indicates the activation of branched-chain amino acids  
543 (BCAA) biosynthesis in response to flavonoids. BCAAs have been shown to have  
544 an essential role in the formation of effective symbiosis between the beta-rhizobia  
545 *Paraburkholderia phyamtum* STM815, and *Cupriavidus taiwanensis* LMG19424  
546 with *Mimosa pudica* plants (Chen et al., 2012). Furthermore, our recent findings  
547 have demonstrated that *C. necator* UYPR2.512 induces the expression of genes  
548 related to BCAAs transport in response to luteolin (Rodríguez-Esperón et al.,  
549 2022). Nonetheless, it should be considered that the statistical support for ilvE  
550 protein is borderline, and further experiments will be needed to clarify its role as  
551 well as the role of BCAAs in the *Cupriavidus sp.* UYMMa02A-plant interaction.

552 A third process influenced by the presence of flavonoids in *Cupriavidus sp.*  
553 UYMMa02A is the possible activation of the glyoxylate cycle (Kornberg, 1966). In  
554 this cycle, isocitrate is converted to succinate and glyoxylate by the enzyme  
555 isocitrate lyase (ICL) followed by the synthesis of malate from glyoxylate and  
556 acetyl-CoA by malate synthase (MS). The glyoxylate cycle enables growth using  
557 C<sub>2</sub> compounds by bypassing the CO<sub>2</sub>-generating steps of the TCA cycle while  
558 generating the necessary products for gluconeogenesis and other biosynthetic  
559 purposes (Dunn et al., 2009). Our hypothesis is supported by the following

1  
2  
3  
4  
5  
6  
7  
8  
9  
10  
11  
12  
13  
14  
15  
16  
17  
18  
19  
20  
21  
22  
23  
24  
25  
26  
27  
28  
29  
30  
31  
32  
33  
34  
35  
36  
37  
38  
39  
40  
41  
42  
43  
44  
45  
46  
47  
48  
49  
50  
51  
52  
53  
54  
55  
56  
57  
58  
59  
60  
61  
62  
63  
64  
65

560 **arguments:** a) The activation of this cycle would explain the observed drop in the  
561 levels of the E2 component of the 2-oxoglutarate dehydrogenase complex, **as**  
562 this enzyme is by-passed **in the cycle** b) **The glyoxylate** cycle would fulfill the  
563 increased **demand for** 2-oxoglutarate, the substrate of the induced aspartate  
564 transaminase/aspartate 4-decarboxylase. Since each turn of the cycle needs two  
565 molecules of acetyl-CoA, the third piece of evidence **supporting** our proposal **is**  
566 the observed increase in the enoyl-CoA hydratase (ECH) levels. This enzyme  
567 catalyzes the second step in the beta-oxidation pathways of fatty acid metabolism  
568 (Moskowitz and Merrick, 1969) and would supply the needed acetyl-CoA  
569 molecules to fuel the glyoxylate cycle. While some of the changes induced by the  
570 assayed flavonoids in *Cupriavidus sp.* UYMMa02A **can** be **linked** to metabolic  
571 processes implicated in the symbiotic interaction between rhizobia and host  
572 plants, additional experiments should be performed to determine the significance  
573 of these findings in interactions involving *Cupriavidus* rhizobial strains.

574 **To improve the simulation of the initial** steps of the symbiotic interaction between  
575 *Cupriavidus sp.* UYMMa02A and *Mimosa pudica*, we implement a co-culture  
576 device. Under these experimental conditions, we observed a **broader** bacterial  
577 response, **as** reflected by the number and distribution of proteins with **altered**  
578 expression among COG categories. Many of the proteins with **changed**  
579 expression were predicted to be **located at** periplasmic or extracellular space,  
580 suggesting that *Cupriavidus sp.* UYMMa02A **undergoes** changes at the  
581 membrane and periplasmic levels during the co-culture conditions. Surface  
582 remodeling has been well documented in many rhizobia models during their  
583 interaction with plant hosts. Variations in exopolysaccharides (EPS),  
584 lipopolysaccharides (LPS), and capsular polysaccharides (KPS) composition are

1  
2  
3  
4  
5  
6  
7  
8  
9  
10  
11  
12  
13  
14  
15  
16  
17  
18  
19  
20  
21  
22  
23  
24  
25  
26  
27  
28  
29  
30  
31  
32  
33  
34  
35  
36  
37  
38  
39  
40  
41  
42  
43  
44  
45  
46  
47  
48  
49  
50  
51  
52  
53  
54  
55  
56  
57  
58  
59  
60  
61  
62  
63  
64  
65

585 required for the **proper** recognition of rhizobial cells by plant hosts, **and for**  
586 **evading the** natural plant immune system (Janczarek, Rachwał, Cieśla, et al.,  
587 2015; Janczarek, Rachwał, Marzec, et al., 2015). Under our experimental  
588 conditions, we observed the augmented expression of FabI, an enoyl-ACP  
589 reductase involved in fatty-acid biosynthesis, which **could reflect** an **upregulation**  
590 **of** lipogenesis for membrane remodeling. Membranes are the **primary** barriers for  
591 **cellular interaction** with the environment, influencing the uptake and efflux of small  
592 molecules. The **observed increase** in OmpC levels in *Cupriavidus sp.*  
593 UYMMa02A during the co-culture could **indicate** the need to **enhance** the  
594 transport of nutrients, signal molecules, or other metabolites across the bacterial  
595 outer membrane. The concomitant levels rise **in** the periplasmic binding  
596 component of an ABC transport system (XylF) putatively involved in  
597 ribose/xylose/arabinose/galactose acquisition, **suggests an** enhanced transport  
598 **capacity** for these sugars. Xylose and ribose have been detected in *M. pudica*  
599 root exudate (Klonowska et al., 2018), **implying** that these sugars may support  
600 *Cupriavidus sp.* UYMMa02A metabolism in the rhizosphere of *M. pudica*. In the  
601 other hand, we also observed an increase in the levels of a protein predicted to  
602 encode the periplasmic adaptor subunit of the resistance-nodule-division (RND)  
603 family efflux transporter. In gram-negative bacteria, RND efflux systems work in  
604 concert with outer membrane porins, like OmpC, to detoxify deleterious  
605 compounds (Nies, 2003; Klonowska et al., 2020). The importance of RND  
606 systems has been demonstrated in many rhizobial species, **where they play a**  
607 **crucial role in** survival and competence in the rhizosphere, affecting nodule  
608 **formation** and nitrogen fixation (Klonowska et al., 2012; Santos et al., 2014).  
609 Moreover, as observed here, some of these systems were shown to be inducible

1  
2  
3  
4  
5  
6  
7  
8  
9  
10  
11  
12  
13  
14  
15  
16  
17  
18  
19  
20  
21  
22  
23  
24  
25  
26  
27  
28  
29  
30  
31  
32  
33  
34  
35  
36  
37  
38  
39  
40  
41  
42  
43  
44  
45  
46  
47  
48  
49  
50  
51  
52  
53  
54  
55  
56  
57  
58  
59  
60  
61  
62  
63  
64  
65

610 both by flavonoids and plant host root exudates. Similarly, Klonowska and  
611 collaborators found that *Cupriavidus taiwanensis* LMG19424 and  
612 *Paraburkholderia phymatum* STM815 RND systems are induced by *M. pudica*  
613 root exudates (Klonowska et al., 2018). Our results suggest that this system  
614 would also be important for the growth of *Cupriavidus sp.* UYMMa02A in the  
615 presence of *M. pudica* root exudates. As mentioned, one role for these efflux  
616 systems is the detoxification of harmful compounds. In that sense, the RAST  
617 annotation server indicates that the identified protein would be a membrane  
618 fusion protein of the CzcB family, which is part of the CzcCBA Heavy metal efflux  
619 (HME) RND system (Janssen et al., 2010). CzcCBA systems were first described  
620 in *C. metallidurans* CH34 and shown to confer resistance to Co, Zn, and Cd. Our  
621 evidence suggests that *Cupriavidus sp.* UYMMa02A activates the extrusion of  
622 metals from its cytoplasm, perhaps preventing the formation of reactive oxygen  
623 species (ROS). The increase in *Cupriavidus sp.* UYMMa02A peroxiredoxin levels  
624 support the hypothesis that ROS are formed during this interaction. Peroxiredoxin  
625 is a periplasmic protein implicated in the detoxification of ROS and peroxynitrite,  
626 also detected in *Rhizobium leguminosarum*, *C. taiwanensis*, and *P. phymatum*  
627 rhizobial strains growing in the presence of root exudates (Ramachandran et al.,  
628 2011; Klonowska et al., 2018). Another stress-related induced protein is  
629 cyclophilin. Cyclophilins are Peptidyl-prolyl cis/trans isomerases (PPIase, EC:  
630 5.2.1.8) enzymes found in all kingdoms of life. Since these proteins catalyze a  
631 rate-limiting step in protein folding, they play a critical role in protein homeostasis.  
632 Diverse studies have demonstrated the participation of these proteins in signal  
633 transduction, biofilm formation, motility, and adaptation to stress (Skagia et al.,  
634 2016; Dimou et al., 2017; Thomludi et al., 2017). Thomludi and collaborators

1  
2  
3  
4  
5  
6  
7  
8  
9  
10  
11  
12  
13  
14  
15  
16  
17  
18  
19  
20  
21  
22  
23  
24  
25  
26  
27  
28  
29  
30  
31  
32  
33  
34  
35  
36  
37  
38  
39  
40  
41  
42  
43  
44  
45  
46  
47  
48  
49  
50  
51  
52  
53  
54  
55  
56  
57  
58  
59  
60  
61  
62  
63  
64  
65

635 showed that the heterologous expression of the two cyclophilins isoforms of  
636 *Sinorhizobium meliloti* 1021 in *E. coli* enhance bacterial survival under stress  
637 condition, supporting the role of these proteins in stress adaptation in bacteria. In  
638 addition, a PPIase mutant in *Azorhizobium caulinodans* ORS571 impairs its  
639 symbiosis with *Sesbania rostrata*, reducing nodule size and completely  
640 abolishing its nitrogen fixation ability (Suzuki et al., 2007). Along with the increase  
641 in the protein levels of the Efflux RND periplasmic adaptor subunit, peroxiredoxin,  
642 and PPIase, we also observed an increase in the universal stress protein A  
643 (UspA) levels. Universal stress proteins are small cytoplasmic bacterial proteins  
644 whose expression is enhanced when the cell is exposed to diverse stress agents  
645 and has been implicated in cell survival during prolonged exposure to stress  
646 conditions (Nyström and Neidhardt, 1994). Induced expression of genes  
647 encoding proteins of this family has been observed during *Rhizobium*  
648 *leguminosarum* growing in the rhizosphere of pea, alfalfa, and sugar beet  
649 (Ramachandran et al., 2011), as well as in *C. taiwanensis* and *P. phymatum*  
650 growing in the presence of *M. pudica* root exudates (Klonowska et al., 2018).  
651 Altogether, the evidence presented here strongly suggests that during the first  
652 steps of the symbiosis, *Cupriavidus sp.* UYMMa02A is under considerable stress  
653 pressure, a common feature in rhizobia-legumes symbiosis.  
654 Finally, we were able to detect the induction of proteins with the potential to  
655 transduce host-secreted signals, such as the protein kinase PrkA protein and the  
656 Nucleotide dikinase (NdK) protein. PrkA is a member of the conserved  
657 serine/threonine protein kinase family widely distributed among Bacteria,  
658 Archaea, and Eukarya (Stancik et al., 2018). Serine/Threonine kinases (STKs)  
659 act in concert with Serine/Threonine phosphatase (STPs) to introduce or remove

1  
2  
3  
4  
5  
6  
7  
8  
9  
10  
11  
12  
13  
14  
15  
16  
17  
18  
19  
20  
21  
22  
23  
24  
25  
26  
27  
28  
29  
30  
31  
32  
33  
34  
35  
36  
37  
38  
39  
40  
41  
42  
43  
44  
45  
46  
47  
48  
49  
50  
51  
52  
53  
54  
55  
56  
57  
58  
59  
60  
61  
62  
63  
64  
65

660 phosphate modifications in proteins at these residues. Reversible protein  
661 phosphorylation is one of the main mechanisms allowing bacteria to respond to  
662 environmental stimuli. Post-translational phosphorylation/dephosphorylation  
663 influences the activity of modified proteins by inducing conformational changes  
664 and regulating protein-protein interactions. Thus, STKs and STPs influence many  
665 different signal transduction pathways in bacteria. In *Rhizobium leguminosarum*,  
666 disruption of the *pssZ* gene, encoding an STK, impacts exopolysaccharide  
667 synthesis, surface properties, and symbiosis with clover (Lipa et al., 2018).  
668 Despite this example, very few studies address the role of STKs in the symbiosis  
669 between rhizobia and legumes. The induction of the *Cupriavidus sp.* UYMMa02A  
670 PrkA in the presence of the host plant *Mimosa pudica*, suggests that this STK  
671 could have an important role during the initial steps of the symbiotic interaction  
672 and demands additional studies to determine its precise role.

673 On the other hand, Ndk s are housekeeping enzymes whose primary role is  
674 maintaining the cellular homeostasis of nucleoside triphosphate (NTP) and their  
675 deoxy derivatives (dNTPs) pools by catalyzing the reversible  $\gamma$ -phosphate  
676 transfer from NTPs (or dNTPs) to NDPs (or dNDPs) (Berg and Joklik, 1953). In  
677 bacteria, the transfer of high-energy phosphates occurs by a ping-pong  
678 mechanism that involves the formation of a phosphor-histidine intermediate at a  
679 conserved histidine residue (Lascu and Gonin, 2000). Moreover, it has been  
680 shown that His-Phosphorylated Ndk s can phosphorylate other proteins at  
681 histidine residues modulating their activities, and affecting a myriad of bacterial  
682 processes (Lu et al., 1996; Attwood and Wieland, 2015). For example, the *E. coli*  
683 Ndk can transfer its phosphate to the sensor proteins EnvZ and CheA, and then  
684 the phosphorylated kinases transfer the high-energy phosphate to their cognate

1  
2  
3  
4  
5  
6  
7  
8  
9  
10  
11  
12  
13  
14  
15  
16  
17  
18  
19  
20  
21  
22  
23  
24  
25  
26  
27  
28  
29  
30  
31  
32  
33  
34  
35  
36  
37  
38  
39  
40  
41  
42  
43  
44  
45  
46  
47  
48  
49  
50  
51  
52  
53  
54  
55  
56  
57  
58  
59  
60  
61  
62  
63  
64  
65

685 response regulators OmpR and CheY, respectively, which are implicated in  
686 osmosis and chemical sensing (Lu et al., 1996). In other bacteria Ndk homologs  
687 have been implicated in the regulation of biofilms formation, the function of type  
688 3 secretion systems, the modulation of quorum sensing, and the response to  
689 oxidative stress, **playing** a critical role in bacteria and host interactions (Yu et al.,  
690 2017). Interestingly, in some bacteria, Ndk can also be found extracellular and  
691 membrane-associated. In *P. aeruginosa*, it has been observed that membrane-  
692 associated Ndk correlates with the status of bacterial growth (Shankar et al.,  
693 1996). **Analysis** of the *Cupriavidus sp.* UYMMa02A Ndk sequence **suggests** that  
694 this protein could have both intracellular and periplasmic locations. The results  
695 presented here, suggest that this protein would be involved in the interaction  
696 between the rhizobial *Cupriavidus sp.* UYMMa02A and the plant host *Mimosa*  
697 *putica*. Further experiments are needed to determine the exact role of this protein  
698 in the interaction, **as** the role of Ndks in beneficial plant-bacteria interaction has  
699 not been studied in detail.

## 700 **Conclusions**

701 The genome of *Cupriavidus sp.* strain UYMMa02A encodes a conserved  
702 symbiotic island **that includes** a complete *nodDBCIJHASUQ* **gene cluster with a**  
703 *nod*-box sequence in the promoter region of *nodB*. However, no induction of the  
704 *Cupriavidus sp.* UYMMa02A *nod* genes was evidenced in **response to** pure  
705 flavonoids or *Mimosa spp.* root exudates. These results suggest that *Cupriavidus*  
706 *sp.* UYMMa02A may employ Nod-independent mechanisms **to stablish**  
707 symbiosis. **Using** a quantitative proteomic approach, we **detected significant**  
708 proteomic changes in *Cupriavidus sp.* UYMMa02A when **exposed** to flavonoids



1  
2  
3  
4  
5  
6  
7  
8  
9  
10  
11  
12  
13  
14  
15  
16  
17  
18  
19  
20  
21  
22  
23  
24  
25  
26  
27  
28  
29  
30  
31  
32  
33  
34  
35  
36  
37  
38  
39  
40  
41  
42  
43  
44  
45  
46  
47  
48  
49  
50  
51  
52  
53  
54  
55  
56  
57  
58  
59  
60  
61  
62  
63  
64  
65

709 or root exudates. Twenty-four differentially expressed proteins were identified  
710 covering diverse bacterial processes ranging from basic metabolism and  
711 transport functions to stress response and signal transduction. In the presence of  
712 the plant host, the major bacterial responses were related to amino acid  
713 metabolism and oxidative stress, which are common features in many rhizobia-  
714 legume interactions. Besides this, the increased levels of the proteins PrkA and  
715 Ndk proteins during the co-culture conditions indicated the involvement of these  
716 versatile proteins in the symbiotic interaction. While further research is necessary  
717 to determine the precise roles of the identified proteins, our study presents a new  
718 model for interrogating the symbiotic interaction between beta-rhizobia and plant  
719 hosts.

720 References:

- 721 Amadou, C., Pascal, G., and Mangenot, S. (2008) Genome sequence of the  $\beta$ -  
722 rhizobium *Cupriavidus taiwanensis* and comparative genomics of rhizobia.  
723 *Genome Res.* **18**: 1472–1483.
- 724 Andam, C.P., Mondo, S.J., and Parker, M.A. (2007) Monophyly of *nodA* and  
725 *nifH* genes across Texan and Costa Rican populations of *Cupriavidus*  
726 nodule symbionts. *Appl. Environ. Microbiol.* **73**: 4686–4690.
- 727 Andrews, M. and Andrews, M.E. (2017) Specificity in legume-rhizobia  
728 symbioses. *Int. J. Mol. Sci.* **18**:
- 729 Attwood, P. V. and Wieland, T. (2015) Nucleoside diphosphate kinase as  
730 protein histidine kinase. *Naunyn. Schmiedeberg's Arch. Pharmacol.* **388**:  
731 153–160.
- 732 Aziz, R.K., Bartels, D., Best, A.A., DeJongh, M., Disz, T., Edwards, R.A., et al.

1  
2  
3  
4  
5  
6  
7  
8  
9  
10  
11  
12  
13  
14  
15  
16  
17  
18  
19  
20  
21  
22  
23  
24  
25  
26  
27  
28  
29  
30  
31  
32  
33  
34  
35  
36  
37  
38  
39  
40  
41  
42  
43  
44  
45  
46  
47  
48  
49  
50  
51  
52  
53  
54  
55  
56  
57  
58  
59  
60  
61  
62  
63  
64  
65

733 (2008) The RAST Server: rapid annotations using subsystems technology.  
734 *BMC Genomics* **9**: 75.

735 Bellés-Sancho, P., Liu, Y., Heiniger, B., von Salis, E., Eberl, L., Ahrens, C.H., et  
736 al. (2022) A novel function of the key nitrogen-fixation activator NifA in  
737 beta-rhizobia: Repression of bacterial auxin synthesis during symbiosis.  
738 *Front. Plant Sci.* **13**..

739 Berg, P. and Joklik, W.K. (1953) Transphosphorylation between Nucleoside  
740 Polyphosphates. *Nature* **172**: 1008–1009.

741 Bontemps, C., Elliott, G.N., Simon, M.F., Dos Reis Júnior, F.B., Gross, E.,  
742 Lawton, R.C., et al. Burkholderia species are ancient symbionts of  
743 legumes. *Mol. Ecol.* **19**: 44–52.

744 Bradford, M.M. (1976) A rapid and sensitive method for the quantitation of  
745 microgram quantities of protein utilizing the principle of protein-dye binding.  
746 *Anal. Biochem.* **72**: 248–254.

747 de Campos, S.B., Lardi, M., Gandolfi, A., Eberl, L., and Pessi, G. (2017)  
748 Mutations in two Paraburkholderia phymatum type VI secretion systems  
749 cause reduced fitness in interbacterial competition. *Front. Microbiol.* **8**..

750 Capela, D., Carrere, S., and Batut, J. (2005) Transcriptome-based identification  
751 of the Sinorhizobium meliloti NodD1 regulon. *Appl. Environ. Microbiol.* **71**:  
752 4910–4913.

753 Caporali, S., De Stefano, A., Calabrese, C., Giovannelli, A., Pieri, M., Savini, I.,  
754 et al. (2022) Anti-Inflammatory and Active Biological Properties of the  
755 Plant-Derived Bioactive Compounds Luteolin and Luteolin 7-Glucoside.  
756 *Nutrients* **14**: 1–19.

757 Chen, C.C., Chou, T.L., and Lee, C.Y. (2000) Cloning, expression and

1  
2  
3  
4  
5  
6  
7  
8  
9  
10  
11  
12  
13  
14  
15  
16  
17  
18  
19  
20  
21  
22  
23  
24  
25  
26  
27  
28  
29  
30  
31  
32  
33  
34  
35  
36  
37  
38  
39  
40  
41  
42  
43  
44  
45  
46  
47  
48  
49  
50  
51  
52  
53  
54  
55  
56  
57  
58  
59  
60  
61  
62  
63  
64  
65

758 characterization of L-aspartate  $\beta$ -decarboxylase gene from *Alcaligenes*  
759 *faecalis* CCRC 11585. *J. Ind. Microbiol. Biotechnol.* **25**: 132–140.

760 Chen, W.-M., Moulin, L., Bontemps, C., Vandamme, P., Béna, G., and Boivin-  
761 Masson, C. (2003) Legume symbiotic nitrogen fixation by beta-  
762 proteobacteria is widespread in nature. *J. Bacteriol.* **185**: 7266–7272.

763 Chen, W.-M., Prell, J., James, E.K., Sheu, D.-S., and Sheu, S.-Y. (2012)  
764 Biosynthesis of branched-chain amino acids is essential for effective  
765 symbioses between betarhizobia and *Mimosa pudica*. *Microbiology* **158**:  
766 1758–66.

767 Chen, W., Laevens, S., Lee, T., Coenye, T., Vos, P. De, Mergeay, M., and  
768 Vandamme, P. (2001) *Ralstonia taiwanensis* sp. nov., isolated from root  
769 nodules of *Mimosa* species and sputum of a cystic fibrosis patient. 1729–  
770 1735.

771 Cheng, C.-S., Su, C.-W., Chang, W.-C., and Huang, K.-C. (2014) CELLO2GO:  
772 A Web Server for Protein subCELLular LOcalization Prediction with  
773 Functional Gene Ontology Annotation. *PLoS One* **9**: 99368.

774 Cunnac, S., Boucher, C., and Genin, S. (2004) Characterization of the cis-  
775 acting regulatory element controlling HrpB-mediated activation of the type  
776 III secretion system and effector genes in *Ralstonia solanacearum*. *J.*  
777 *Bacteriol.* **186**: 2309–2318.

778 Dall’Agnol, R.F., Bournaud, C., de Faria, S.M., Bena, G., Moulin, L., and  
779 Hungria, M. (2017) Genetic diversity of symbiotic Paraburkholderia species  
780 isolated from nodules of *Mimosa pudica* (L.) and *Phaseolus vulgaris* (L.)  
781 grown in soils of the Brazilian Atlantic Forest (Mata Atlantica). *Ecol* **93**.

782 diCenzo, G.C., Zamani, M., Checcucci, A., Fondi, M., Griffiths, J.S., Finan, T.M.,

1  
2  
3  
4  
5  
6  
7  
8  
9  
10  
11  
12  
13  
14  
15  
16  
17  
18  
19  
20  
21  
22  
23  
24  
25  
26  
27  
28  
29  
30  
31  
32  
33  
34  
35  
36  
37  
38  
39  
40  
41  
42  
43  
44  
45  
46  
47  
48  
49  
50  
51  
52  
53  
54  
55  
56  
57  
58  
59  
60  
61  
62  
63  
64  
65

783 and Mengoni, A. (2019) Multidisciplinary approaches for studying  
784 rhizobium–legume symbioses. *Can. J. Microbiol.* **65**: 1–33.

785 Dimou, M., Venieraki, A., and Katinakis, P. (2017) Microbial cyclophilins:  
786 specialized functions in virulence and beyond. *World J. Microbiol.*  
787 *Biotechnol.* **33**: 1–8.

788 Dunn, M.F., Ramírez-Trujillo, J.A., and Hernández-Lucas, I. (2009) Major roles  
789 of isocitrate lyase and malate synthase in bacterial and fungal  
790 pathogenesis. *Microbiology* **155**: 3166–3175.

791 Estrada-de los Santos, P., Palmer, M., Chávez-Ramírez, B., Beukes, C.,  
792 Steenkamp, E.T., Briscoe, L., et al. (2018) Whole genome analyses  
793 suggests that Burkholderia sensu lato contains two additional novel genera  
794 (Mycetohabitans gen. nov., and Trinickia gen. nov.): Implications for the  
795 evolution of diazotrophy and nodulation in the Burkholderiaceae. *Genes*  
796 *(Basel)*. **9**:

797 Fagorzi, C., Bacci, G., Huang, R., Cangioli, L., Checcucci, A., Fini, M., et al.  
798 (2021) Nonadditive Transcriptomic Signatures of Genotype-by-Genotype  
799 Interactions during the Initiation of Plant-Rhizobium Symbiosis. *mSystems*  
800 **6**:

801 Gambino, M. and Cappitelli, F. (2016) Mini-review: Biofilm responses to  
802 oxidative stress. *Biofouling* **32**: 167–178.

803 Garau, G., Yates, R.J., Deiana, P., and Howieson, J.G. (2009) Novel strains of  
804 nodulating Burkholderia have a role in nitrogen fixation with papilionoid  
805 herbaceous legumes adapted to acid, infertile soils. *Soil Biol. Biochem.* **41**:  
806 125–134.

807 Gehlot, H.S., Tak, N., Kaushik, M., Mitra, S., Chen, W.-M., Poweleit, N., et al.

1  
2  
3  
4  
5  
6  
7  
8  
9  
10  
11  
12  
13  
14  
15  
16  
17  
18  
19  
20  
21  
22  
23  
24  
25  
26  
27  
28  
29  
30  
31  
32  
33  
34  
35  
36  
37  
38  
39  
40  
41  
42  
43  
44  
45  
46  
47  
48  
49  
50  
51  
52  
53  
54  
55  
56  
57  
58  
59  
60  
61  
62  
63  
64  
65

808 (2013) An invasive Mimosa in India does not adopt the symbionts of its  
809 native relatives. *Ann. Bot.* **112**: 179–96.

810 Gil, M., Lima, A., Rivera, B., Rossello, J., Urdániz, E., Cascioferro, A., et al.  
811 (2019) New substrates and interactors of the mycobacterial  
812 Serine/Threonine protein kinase PknG identified by a tailored interactomic  
813 approach. *J. Proteomics* **192**: 321–333.

814 Giraud, E., Moulin, L., Vallenet, D., Barbe, V., Cytryn, E., Avarre, J.-C., et al.  
815 (2007) Legumes symbioses: absence of Nod genes in photosynthetic  
816 bradyrhizobia. *Science* **316**: 1307–12.

817 Gourion, B., Berrabah, F., Ratet, P., and Stacey, G. (2015) Rhizobium-legume  
818 symbioses: The crucial role of plant immunity. *Trends Plant Sci.* **20**: 186–  
819 194.

820 Guha, S., Molla, F., Sarkar, M., Ibañez, F., Fabra, A., and DasGupta, M. (2022)  
821 Nod factor-independent “crack-entry” symbiosis in dalbergoid legume  
822 *Arachis hypogaea*. *Environ. Microbiol.* **24**: 2732–2746.

823 Howieson, J.G., De Meyer, S.E., Vivas-Marfisi, A., Ratnayake, S., Ardley, J.K.,  
824 and Yates, R.J. (2013) Novel Burkholderia bacteria isolated from *Lebeckia*  
825 *ambigua* - A perennial suffrutescent legume of the fynbos. *Soil Biol.*  
826 *Biochem.* **60**: 55–64.

827 Howieson, J.G., Robson, A.D., and Ewing, M.A. (1993) External phosphate and  
828 calcium concentrations, and Ph, but not the products of rhizobial nodulation  
829 genes, affect the attachment of rhizobium meliloti to roots of annual  
830 medics. *Soil Biol. Biochem.* **25**: 567–573.

831 Huergo, L.F. and Dixon, R. (2015) The Emergence of 2-Oxoglutarate as a  
832 Master Regulator Metabolite. *Microbiol. Mol. Biol. Rev.* **79**: 419–435.

1  
2  
3  
4  
5  
6  
7  
8  
9  
10  
11  
12  
13  
14  
15  
16  
17  
18  
19  
20  
21  
22  
23  
24  
25  
26  
27  
28  
29  
30  
31  
32  
33  
34  
35  
36  
37  
38  
39  
40  
41  
42  
43  
44  
45  
46  
47  
48  
49  
50  
51  
52  
53  
54  
55  
56  
57  
58  
59  
60  
61  
62  
63  
64  
65

833 Huerta-Cepas, J., Szklarczyk, D., Forslund, K., Cook, H., Heller, D., Walter,  
834 M.C., et al. (2016) eggNOG 4.5: a hierarchical orthology framework with  
835 improved functional annotations for eukaryotic, prokaryotic and viral  
836 sequences. *Nucleic Acids Res.* **44**: 286–293.

837 Hungria, M., Joseph, C.M., and Phillips, D. a (1991) Rhizobium nod Gene  
838 Inducers Exuded Naturally from Roots of Common Bean (*Phaseolus*  
839 *vulgaris* L.). *Plant Physiol.* **97**: 759–764.

840 Iriarte, A., Platero, R., Romero, V., Fabiano, E., and Sotelo-Silveira, J.R. (2016)  
841 Draft genome sequence of *Cupriavidus* UYMMa02A, a novel beta-  
842 rhizobium species. *Genome Announc.* **4**: e01258-16.

843 Janczarek, M., Rachwał, K., Cieśla, J., Ginalska, G., and Bieganowski, A.  
844 (2015) Production of exopolysaccharide by *Rhizobium leguminosarum* bv.  
845 *trifolii* and its role in bacterial attachment and surface properties. *Plant Soil*  
846 **388**: 211–227.

847 Janczarek, M., Rachwał, K., Marzec, A., Grządziel, J., and Palusińska-Szyszc,  
848 M. (2015) Signal molecules and cell-surface components involved in early  
849 stages of the legume–rhizobium interactions. *Appl. Soil Ecol.* **85**: 94–113.

850 Janssen, P.J., Van Houdt, R., Moors, H., Monsieurs, P., Morin, N., Michaux, A.,  
851 et al. (2010) The Complete Genome Sequence of *Cupriavidus*  
852 *metallidurans* Strain CH34, a Master Survivalist in Harsh and  
853 Anthropogenic Environments. *PLoS One* **5**: e10433.

854 Jiménez-Guerrero, I., Acosta-Jurado, S., del Cerro, P., Navarro-Gómez, P.,  
855 López-Baena, F., Ollero, F., et al. (2017) Transcriptomic Studies of the  
856 Effect of nod Gene-Inducing Molecules in Rhizobia: Different Weapons,  
857 One Purpose. *Genes (Basel)*. **9**: 1.

1  
2  
3  
4  
5  
6  
7  
8  
9  
10  
11  
12  
13  
14  
15  
16  
17  
18  
19  
20  
21  
22  
23  
24  
25  
26  
27  
28  
29  
30  
31  
32  
33  
34  
35  
36  
37  
38  
39  
40  
41  
42  
43  
44  
45  
46  
47  
48  
49  
50  
51  
52  
53  
54  
55  
56  
57  
58  
59  
60  
61  
62  
63  
64  
65

858 Jiménez-Guerrero, I., Acosta-Jurado, S., del Cerro, P., Navarro-Gómez, P.,  
859 López-Baena, F.J., Ollero, F.J., et al. (2018) Transcriptomic studies of the  
860 effect of nod gene-inducing molecules in rhizobia: Different weapons, one  
861 purpose. *Genes (Basel)*. **9**:.

862 Kakimoto, T., Kato, J., Shibatani, T., Nishimura, N., and Chibata, I. (1969)  
863 Crystalline L-Aspartate  $\beta$ -Decarboxylase of *Pseudomonas dacunhae*. *J.*  
864 *Biol. Chem.* **244**: 353–358.

865 Klonowska, A., Chaintreuil, C., Tisseyre, P., Miché, L., Melkonian, R.,  
866 Ducouso, M., et al. (2012) Biodiversity of *Mimosa pudica* rhizobial  
867 symbionts (*Cupriavidus taiwanensis*, *Rhizobium mesoamericanum*) in New  
868 Caledonia and their adaptation to heavy metal-rich soils. *FEMS Microbiol.*  
869 *Ecol.* **81**: 618–635.

870 Klonowska, A., Melkonian, R., Miché, L., Tisseyre, P., and Moulin, L. (2018)  
871 Transcriptomic profiling of *Burkholderia phymatum* STM815, *Cupriavidus*  
872 *taiwanensis* LMG19424 and *Rhizobium mesoamericanum* STM3625 in  
873 response to *Mimosa pudica* root exudates illuminates the molecular basis  
874 of their nodulation competitiveness and symbiotic ev. *BMC Genomics* **19**:  
875 105.

876 Klonowska, A., Moulin, L., Ardley, J.K., Braun, F., Gollagher, M.M., Zandberg,  
877 J.D., et al. (2020) Novel heavy metal resistance gene clusters are present  
878 in the genome of *Cupriavidus neocaledonicus* STM 6070, a new species of  
879 *Mimosa pudica* microsymbiont isolated from heavy-metal-rich mining site  
880 soil. *BMC Genomics* **21**: 214.

881 Kornberg, H.L. (1966) The role and control of the glyoxylate cycle in *Escherichia*  
882 *coli*. *Biochem. J.* **99**: 1–11.

- 1  
2  
3  
4  
5  
6  
7  
8  
9  
10  
11  
12  
13  
14  
15  
16  
17  
18  
19  
20  
21  
22  
23  
24  
25  
26  
27  
28  
29  
30  
31  
32  
33  
34  
35  
36  
37  
38  
39  
40  
41  
42  
43  
44  
45  
46  
47  
48  
49  
50  
51  
52  
53  
54  
55  
56  
57  
58  
59  
60  
61  
62  
63  
64  
65
- 883 Kumar, S., Stecher, G., and Tamura, K. (2016) MEGA7: Molecular Evolutionary  
884 Genetics Analysis Version 7.0 for Bigger Datasets. *Mol. Biol. Evol.* **33**:  
885 1870–1874.
- 886 Laemmli, U. (1970) Cleavage of Structural Proteins during the Assembly of the  
887 Head of Bacteriophage T4. *Nature*.
- 888 Lardi, M., Liu, Y., Purtschert, G., de Campos, S.B., and Pessi, G. (2017)  
889 Transcriptome analysis of *Paraburkholderia phymatum* under Nitrogen  
890 starvation and during symbiosis with *Phaseolus Vulgaris*. *Genes (Basel)*.  
891 **8**.
- 892 Lascu, I. and Gonin, P. (2000) The catalytic mechanism of nucleoside  
893 diphosphate kinases. *J. Bioenerg. Biomembr.* **32**: 237–46.
- 894 Lemaire, B., Dlodlo, O., Chimphango, S., Stirton, C., Schrire, B., Boatwright,  
895 J.S., et al. (2015) Symbiotic diversity, specificity and distribution of rhizobia  
896 in native legumes of the Core Cape Subregion (South Africa). *FEMS*  
897 *Microbiol. Ecol.* **91**: 1–17.
- 898 Lindström, K. and Mousavi, S.A. (2020) Effectiveness of nitrogen fixation in  
899 rhizobia. *Microb. Biotechnol.* **13**: 1314–1335.
- 900 Lipa, P., Vinardell, J.M., Kopcińska, J., Zdybicka-Barabas, A., and Janczarek,  
901 M. (2018) Mutation in the *pssZ* gene negatively impacts exopolysaccharide  
902 synthesis, surface properties, and symbiosis of *Rhizobium leguminosarum*  
903 *bv. trifolii* with clover. *Genes (Basel)*. **9**.
- 904 Liu, X., Wei, S., Wang, F., James, E.K., Guo, X., Zagar, C., et al. (2012)  
905 *Burkholderia* and *Cupriavidus* spp. are the preferred symbionts of *Mimosa*  
906 spp. in Southern China. *FEMS Microbiol. Ecol.* **80**: 417–426.
- 907 Liu, Y., Bellich, B., Hug, S., Eberl, L., Cescutti, P., and Pessi, G. (2020) The



1  
2  
3  
4  
5  
6  
7  
8  
9  
10  
11  
12  
13  
14  
15  
16  
17  
18  
19  
20  
21  
22  
23  
24  
25  
26  
27  
28  
29  
30  
31  
32  
33  
34  
35  
36  
37  
38  
39  
40  
41  
42  
43  
44  
45  
46  
47  
48  
49  
50  
51  
52  
53  
54  
55  
56  
57  
58  
59  
60  
61  
62  
63  
64  
65

908 Exopolysaccharide Cepacian Plays a Role in the Establishment of the  
909 Paraburkholderia phymatum – Phaseolus vulgaris Symbiosis. *Front.*  
910 *Microbiol.* **11**:.  
911 Lu, Q., Park, H., Egger, L.A., and Inouye, M. (1996) Nucleoside-diphosphate  
912 Kinase-mediated Signal Transduction via Histidyl-Aspartyl Phosphorelay  
913 Systems in Escherichia coli. *J. Biol. Chem.* **271**: 32886–32893.  
914 Mailloux, R.J., Bériault, R., Lemire, J., Singh, R., Chénier, D.R., Hamel, R.D.,  
915 and Appanna, V.D. (2007) The tricarboxylic acid cycle, an ancient  
916 metabolic network with a novel twist. *PLoS One* **2**: e690.  
917 Marchetti, M., Capela, D., Glew, M., Cruveiller, S., Chane-Woon-Ming, B., Gris,  
918 C., et al. (2010) Experimental Evolution of a Plant Pathogen into a Legume  
919 Symbiont. *PLoS Biol.* **8**: e1000280.  
920 Marchetti, M., Catrice, O., Batut, J., and Masson-Boivin, C. (2011) Cupriavidus  
921 taiwanensis bacteroids in Mimosa pudica Indeterminate nodules are not  
922 terminally differentiated. *Appl. Environ. Microbiol.* **77**: 2161–4.  
923 Martinez, A. and Kolter, R. (1997) Protection of DNA during oxidative stress by  
924 the nonspecific DNA- binding protein Dps. *J. Bacteriol.* **179**: 5188–5194.  
925 Masson-Boivin, C., Giraud, E., Perret, X., and Batut, J. (2009) Establishing  
926 nitrogen-fixing symbiosis with legumes: how many rhizobium recipes?  
927 *Trends Microbiol.* **17**: 458–66.  
928 Meleady, P. (2018) Two-Dimensional Gel Electrophoresis and 2D-DIGE.  
929 *Methods Mol. Biol.* **1664**: 3–14.  
930 De Meyer, Sofie E, Briscoe, L., Martínez-Hidalgo, P., Agapakis, C.M., de-Los  
931 Santos, P.E., Seshadri, R., et al. (2016) Symbiotic Burkholderia Species  
932 Show Diverse Arrangements of nif/fix and nod Genes and Lack Typical

1  
2  
3  
4  
5  
6  
7  
8  
9  
10  
11  
12  
13  
14  
15  
16  
17  
18  
19  
20  
21  
22  
23  
24  
25  
26  
27  
28  
29  
30  
31  
32  
33  
34  
35  
36  
37  
38  
39  
40  
41  
42  
43  
44  
45  
46  
47  
48  
49  
50  
51  
52  
53  
54  
55  
56  
57  
58  
59  
60  
61  
62  
63  
64  
65

933 High-Affinity Cytochrome cbb3 Oxidase Genes. *Mol. Plant. Microbe.*  
934 *Interact.* **29**: 609–19.

935 De Meyer, Sofie E, Fabiano, E., Tian, R., Van Berkum, P., Seshadri, R., Reddy,  
936 T., et al. (2015) High-quality permanent draft genome sequence of the  
937 *Parapiptadenia rigida*-nodulating *Cupriavidus* sp. strain UYPR2.512. *Stand*  
938 *Genomic Sci* **10**: 13.

939 De Meyer, Sofie E., Parker, M., Van Berkum, P., Tian, R., Seshadri, R., Reddy,  
940 T.B.K., et al. (2015) High-quality permanent draft genome sequence of the  
941 *Mimosa asperata* - nodulating *Cupriavidus* sp. strain AMP6. *Stand.*  
942 *Genomic Sci.* **10**: 9–11.

943 Miché, L., Moulin, L., Chaintreuil, C., Contreras-Jimenez, J.L., Munive-  
944 Hernández, J.A., del Carmen Villegas-Hernandez, M., et al. (2010)  
945 Diversity analyses of *Aeschynomene* symbionts in Tropical Africa and  
946 Central America reveal that nod-independent stem nodulation is not  
947 restricted to photosynthetic bradyrhizobia. *Environ. Microbiol.* **12**: 2152–  
948 2164.

949 Miller, J.H. (1972) Assay of B-galactosidase In: Experiments in molecular  
950 genetics Cold Spring Harbor Laboratory Press, Cold Spring Harbor, NY.

951 Moskowitz, G.J. and Merrick, J.M. (1969) Metabolism of poly- $\beta$ -hydroxybutyrate.  
952 II. Enzymic synthesis of D-(-)- $\beta$ -hydroxybutyryl coenzyme A by an enoyl  
953 hydratase from *Rhodospirillum rubrum*. *Biochemistry* **8**: 2748–2755.

954 Moulin, L., Klonowska, A., Caroline, B., Booth, K., Vriezen, J. a C., Melkonian,  
955 R., et al. (2014) Complete Genome sequence of *Burkholderia phymatum*  
956 STM815(T), a broad host range and efficient nitrogen-fixing symbiont of  
957 *Mimosa* species. *Stand. Genomic Sci.* **9**: 763–74.

1  
2  
3  
4  
5  
6  
7  
8  
9  
10  
11  
12  
13  
14  
15  
16  
17  
18  
19  
20  
21  
22  
23  
24  
25  
26  
27  
28  
29  
30  
31  
32  
33  
34  
35  
36  
37  
38  
39  
40  
41  
42  
43  
44  
45  
46  
47  
48  
49  
50  
51  
52  
53  
54  
55  
56  
57  
58  
59  
60  
61  
62  
63  
64  
65

958 Mozejko-Ciesielska, J. and Mostek, A. (2019) A 2D-DIGE-based proteomic  
959 analysis brings new insights into cellular responses of *Pseudomonas putida*  
960 KT2440 during polyhydroxyalkanoates synthesis. *Microb. Cell Fact.* **18**: 1–  
961 13.

962 Nies, D.H. (2003) Efflux-mediated heavy metal resistance in prokaryotes. *FEMS*  
963 *Microbiol. Rev.* **27**: 313–339.

964 Nyström, T. and Neidhardt, F.C. (1994) Expression and role of the universal  
965 stress protein, UspA, of *Escherichia coli* during growth arrest. *Mol.*  
966 *Microbiol.* **11**: 537–44.

967 Oldroyd, G.E.D., Murray, J.D., Poole, P.S., and Downie, J.A. (2011) The rules  
968 of engagement in the legume-rhizobial symbiosis. *Annu. Rev. Genet.* **45**:  
969 119–44.

970 Orban, K. and Finkel, S.E. (2022) Dps Is a Universally Conserved Dual-Action  
971 DNA-Binding and Ferritin Protein. *J. Bacteriol.* **204**: 1–23.

972 Parker, M.A., Wurtz, A.K., and Paynter, Q. (2007) Nodule Symbiosis of Invasive  
973 *Mimosa pigra* in Australia and in Ancestral Habitats: A Comparative  
974 Analysis. *Biol. Invasions* **9**: 127–138.

975 Pereira-Gómez, M., Ríos, C., Zabaleta, M., Lagurara, P., Galvalisi, U., Iccardi,  
976 P., et al. (2020) Native legumes of the Farrapos protected area in Uruguay  
977 establish selective associations with rhizobia in their natural habitat. *Soil*  
978 *Biol. Biochem.* **148**: 107854.

979 Platero, R., James, E.K., Rios, C., Iriarte, A., Sandes, L., Zabaleta, M., et al.  
980 (2016) Novel *Cupriavidus* Strains Isolated from Root Nodules of Native  
981 Uruguayan *Mimosa* Species. *Appl. Environ. Microbiol.* **82**: 3150–3164.

982 Prell, J. and Poole, P. (2006) Metabolic changes of rhizobia in legume nodules.

1  
2  
3  
4  
5  
6  
7  
8  
9  
10  
11  
12  
13  
14  
15  
16  
17  
18  
19  
20  
21  
22  
23  
24  
25  
26  
27  
28  
29  
30  
31  
32  
33  
34  
35  
36  
37  
38  
39  
40  
41  
42  
43  
44  
45  
46  
47  
48  
49  
50  
51  
52  
53  
54  
55  
56  
57  
58  
59  
60  
61  
62  
63  
64  
65

983 *Trends Microbiol.* **14**: 161–8.

984 Prell, J., White, J.P., Bourdes, A., Bunnewell, S., Bongaerts, R.J., and Poole,  
985 P.S. (2009) Legumes regulate Rhizobium bacteroid development and  
986 persistence by the supply of branched-chain amino acids. *Proc. Natl. Acad.*  
987 *Sci. U. S. A.* **106**: 12477–12482.

988 Ramachandran, V.K., East, A.K., Karunakaran, R., Downie, J.A., and Poole,  
989 P.S. (2011) Adaptation of Rhizobium leguminosarum to pea, alfalfa and  
990 sugar beet rhizospheres investigated by comparative transcriptomics.  
991 *Genome Biol.* **12**..

992 dos Reis, F.B., Simon, M.F., Gross, E., Boddey, R.M., Elliott, G.N., Neto, N.E.,  
993 et al. (2010) Nodulation and nitrogen fixation by Mimosa spp. in the  
994 Cerrado and Caatinga biomes of Brazil. *New Phytol.* **186**: 934–946.

995 Rodríguez-Esperón, M.C., Eastman, G., Sandes, L., Garabato, F., Eastman, I.,  
996 Iriarte, A., et al. (2022) Genomics and transcriptomics insights into luteolin  
997 effects on the beta-rhizobial strain Cupriavidus necator UYPR2.512.  
998 *Environ. Microbiol.* **24**: 240–264.

999 Saad, M.M., Crèvecoeur, M., Masson-Boivin, C., and Perret, X. (2012) The type  
1000 3 protein secretion system of Cupriavidus taiwanensis strain LMG19424  
1001 compromises symbiosis with Leucaena leucocephala. *Appl. Environ.*  
1002 *Microbiol.* **78**: 7476–7479.

1003 Salehi, B., Venditti, A., Sharifi-Rad, M., Kręgiel, D., Sharifi-Rad, J., Durazzo, A.,  
1004 et al. (2019) The therapeutic potential of Apigenin. *Int. J. Mol. Sci.* **20**..

1005 Sambrook, J., Fritsch, E.F., and Maniatis, T. (1989) Molecular cloning: a  
1006 laboratory manual. *Mol. cloning a Lab. manual.*

1007 Santos, M.R., Marques, A.T., Becker, J.D., and Moreira, L.M. (2014) The

- 1008 sinorhizobium meliloti emrr regulator is required for efficient colonization of  
1009 medicago sativa root nodules. *Mol. Plant-Microbe Interact.* **27**: 388–399.
- 1010 Schlaman, H.R.M., Okker, R.J.H., and Lugtenberg, B.J.J. (1992) Regulation of  
1011 nodulation gene expression by nodD in rhizobia. *J. Bacteriol.* **174**: 5177–  
1012 5182.
- 1013 Schmidt, P.E., Broughton, W.J., and Werner, D. (1994) Nod Factors of  
1014 Bradyrhizobium-Japonicum and Rhizobium Sp Ngr234 Induce Flavonoid  
1015 Accumulation in Soybean Root Exudate. *Mol. Plant-Microbe Interact.* **7**:  
1016 384–390.
- 1017 Shankar, S., Kamath, S., and Chakrabarty, A.M. (1996) Two forms of the  
1018 nucleoside diphosphate kinase of Pseudomonas aeruginosa 8830: Altered  
1019 specificity of nucleoside triphosphate synthesis by the cell membrane-  
1020 associated form of the truncated enzyme. *J. Bacteriol.* **178**: 1777–1781.
- 1021 Skagia, A., Zografou, C., Vezyri, E., Venieraki, A., Katinakis, P., and Dimou, M.  
1022 (2016) Cyclophilin PpiB is involved in motility and biofilm formation via its  
1023 functional association with certain proteins. *Genes to Cells* **21**: 833–851.
- 1024 Stancik, I.A., Šestak, M.S., Ji, B., Axelson-Fisk, M., Franjevic, D., Jers, C., et al.  
1025 (2018) Serine/Threonine Protein Kinases from Bacteria, Archaea and  
1026 Eukarya Share a Common Evolutionary Origin Deeply Rooted in the Tree  
1027 of Life. *J. Mol. Biol.* **430**: 27–32.
- 1028 Suzuki, S., Aono, T., Lee, K.B., Suzuki, T., Liu, C. Te, Miwa, H., et al. (2007)  
1029 Rhizobial factors required for stem nodule maturation and maintenance in  
1030 Sesbania rostrata-Azorhizobium caulinodans ORS571 symbiosis. *Appl.*  
1031 *Environ. Microbiol.* **73**: 6650–6659.
- 1032 Taulé, C., Zabaleta, M., Mareque, C., Platero, R., Sanjurjo, L., Sicardi, M., et al.

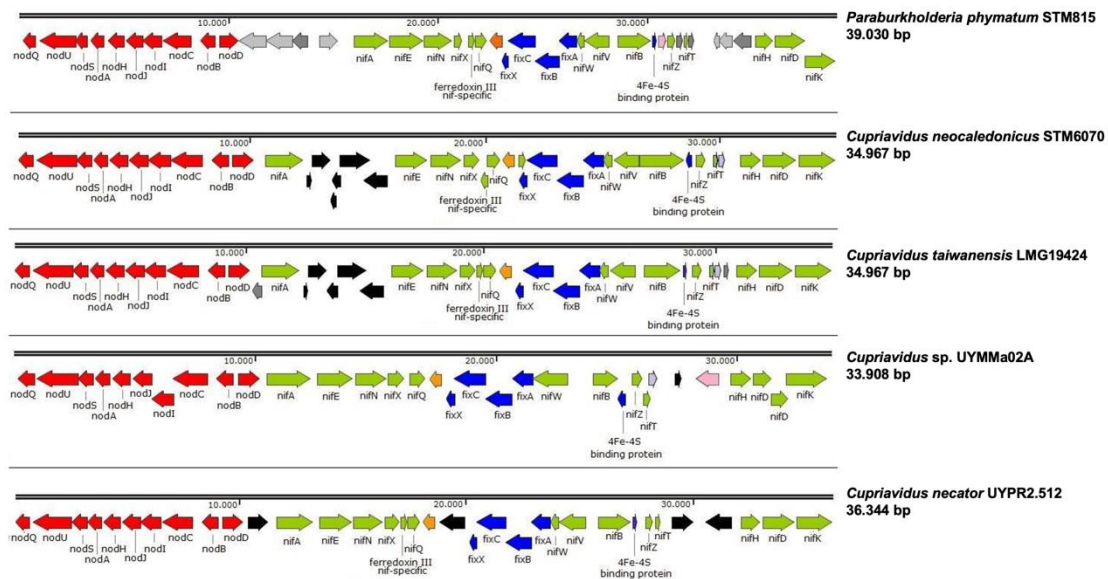
1033 (2012) New betaproteobacterial *Rhizobium* strains able to efficiently  
 1034 nodulate *Parapiptadenia rigida* (Benth.) Brenan. *Appl. Environ. Microbiol.*  
 1035 **78**: 1692–700.

1036 Thomloui, E.-E., Skagia, A., Venieraki, A., Katinakis, P., and Dimou, M. (2017)  
 1037 Functional analysis of the two cyclophilin isoforms of *Sinorhizobium*  
 1038 *meliloti*. *World J. Microbiol. Biotechnol.* **33**: 28.

1039 Wu, P.S., Yen, J.H., Kou, M.C., and Wu, M.J. (2015) Luteolin and apigenin  
 1040 attenuate 4-hydroxy- 2-nonenal-mediated cell death through modulation of  
 1041 UPR, Nrf2-ARE and MAPK pathways in PC12 cells. *PLoS One* **10**: 1–23.

1042 Yu, H., Rao, X., and Zhang, K. (2017) Nucleoside diphosphate kinase (Ndk): A  
 1043 pleiotropic effector manipulating bacterial virulence and adaptive  
 1044 responses. *Microbiol. Res.* **205**: 125–134.

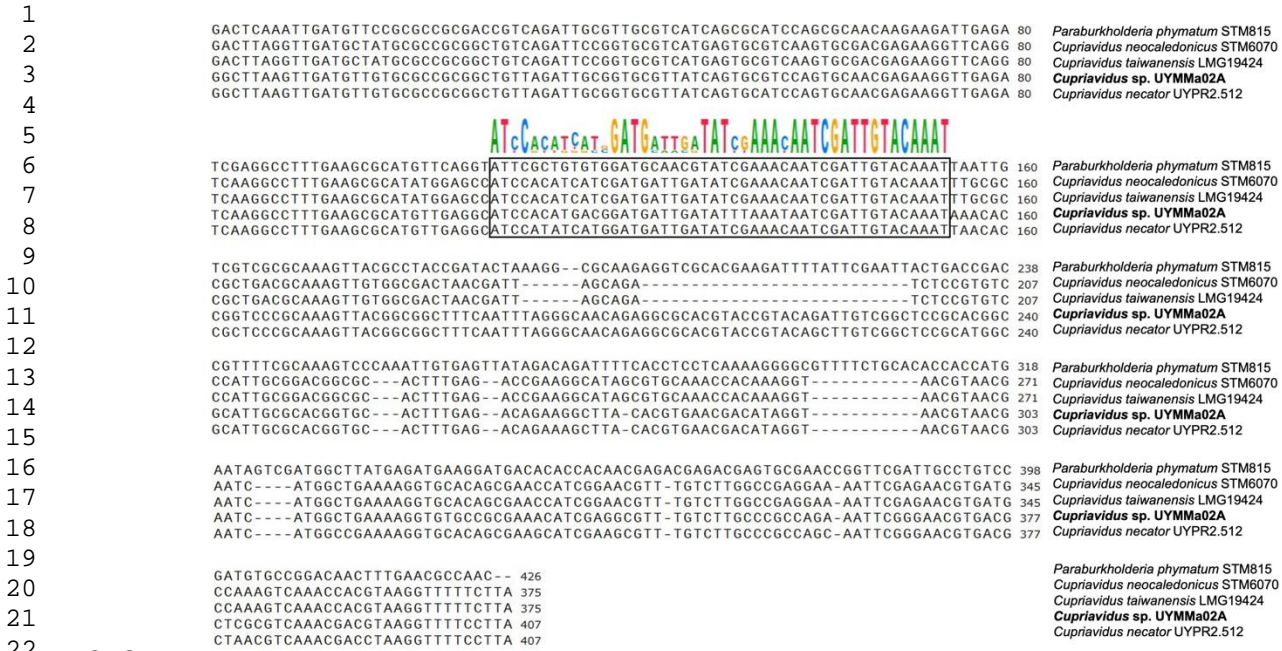
1045 Zheng, J., Wang, R., Liu, R., Chen, J., Wei, Q., Wu, X., et al. (2017) Immunome  
 1046 Research The Structure and Evolution of Beta-Rhizobial Symbiotic Genes  
 1047 Deduced from Their Complete Genomes. **13**: 131:



1048  
 1049 Figure 1: Comparison of symbiotic islands of different beta-rhizobia. The

1050 size of each symbiotic island is indicated below strain names. Genes  
1  
2 1051 belonging to the *nod/nif/fix* operons are coloured in red/green/blue  
3  
4 1052 respectively, and transposons-related genes are coloured in black. Other  
5  
6 1053 colours represent genes that do not belong to the aforementioned operons.  
7  
8  
9 1054  
10  
11  
12  
13  
14  
15  
16  
17  
18  
19  
20  
21  
22  
23  
24  
25  
26  
27  
28  
29  
30  
31  
32  
33  
34  
35  
36  
37  
38  
39  
40  
41  
42  
43  
44  
45  
46  
47  
48  
49  
50  
51  
52  
53  
54  
55  
56  
57  
58  
59  
60  
61  
62  
63  
64  
65

1055

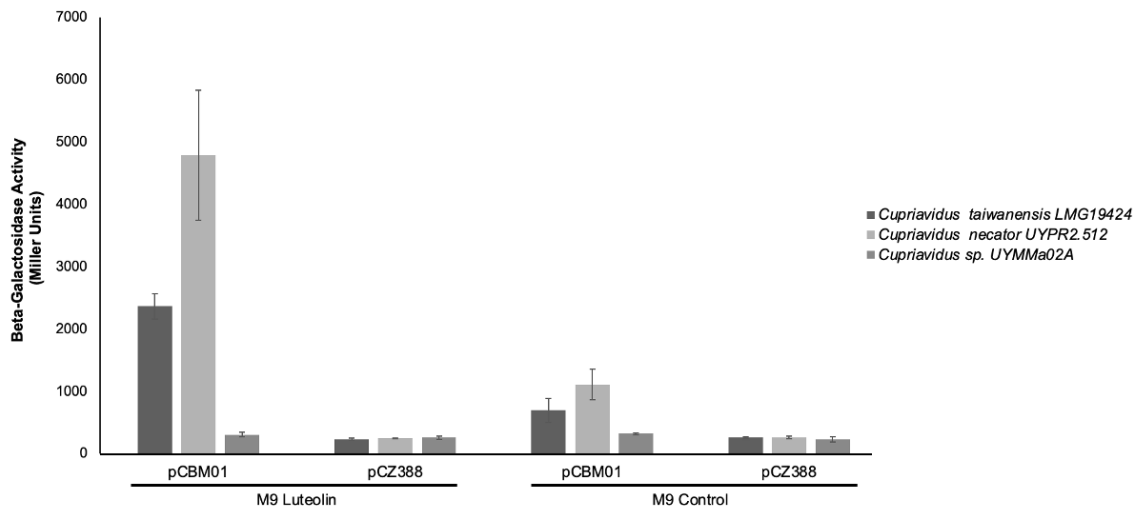


1056

1057 Figure 2: Sequence alignment of the *nodB-nodD* sequence in different Beta-  
1058 rhizobia strains. Aligned sequences include the intergenic region between *nodB*  
1059 and *nodD* and the first 100 bp of both genes. The black rectangle indicates *nod*-  
1060 box localization. Conserved motifs are highlighted in colour letters.

1061





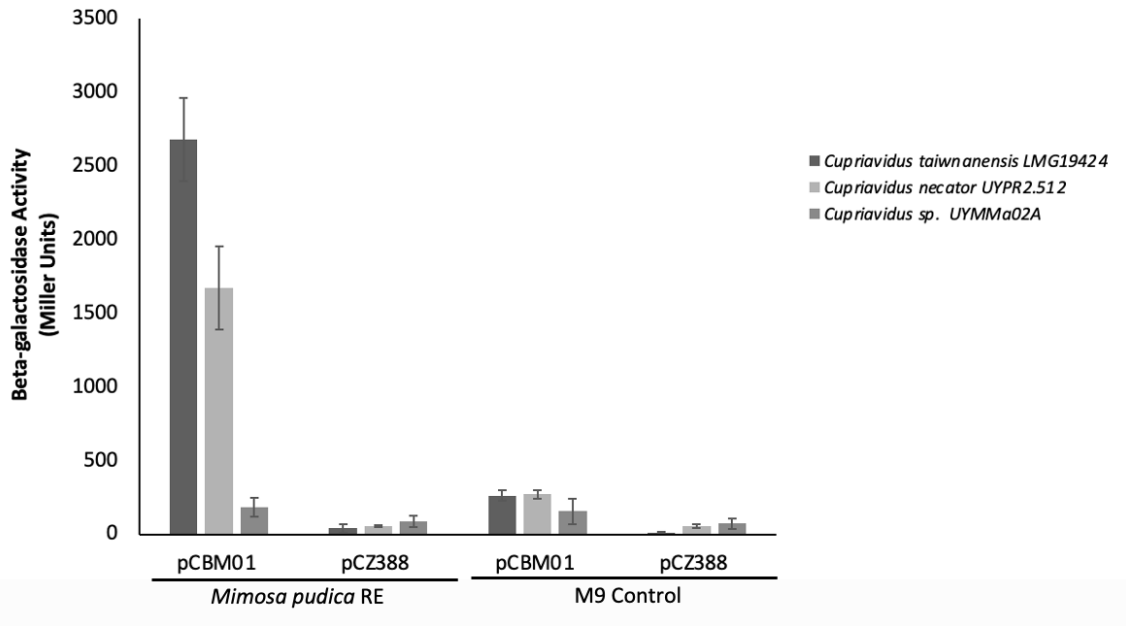
1062

1063 Figure 3. Expression of the *pnodB*<sub>19424</sub>-*lacZ* fusion in *Cupriavidus taiwanensis*

1064 LMG 19424, *Cupriavidus necator* UYPR2.512, and *Cupriavidus sp.* UYMMa02A

1065 in response to luteolin.

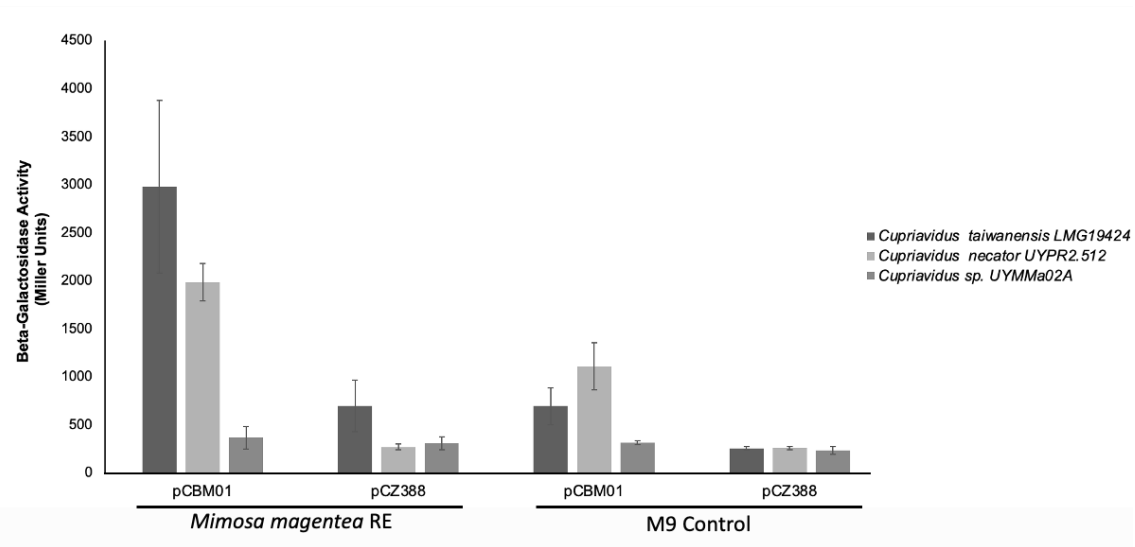
1066



1067

1068 Figure 4. Expression of the *pnodB*<sub>19424</sub>-*lacZ* fusion in *Cupriavidus taiwanensis*  
 1069 LMG19424, *Cupriavidus necator* UYPR2.512, and *Cupriavidus sp.* UYMMa02A  
 1070 in response to *Mimosa pudica* root exudates (RE).

1071

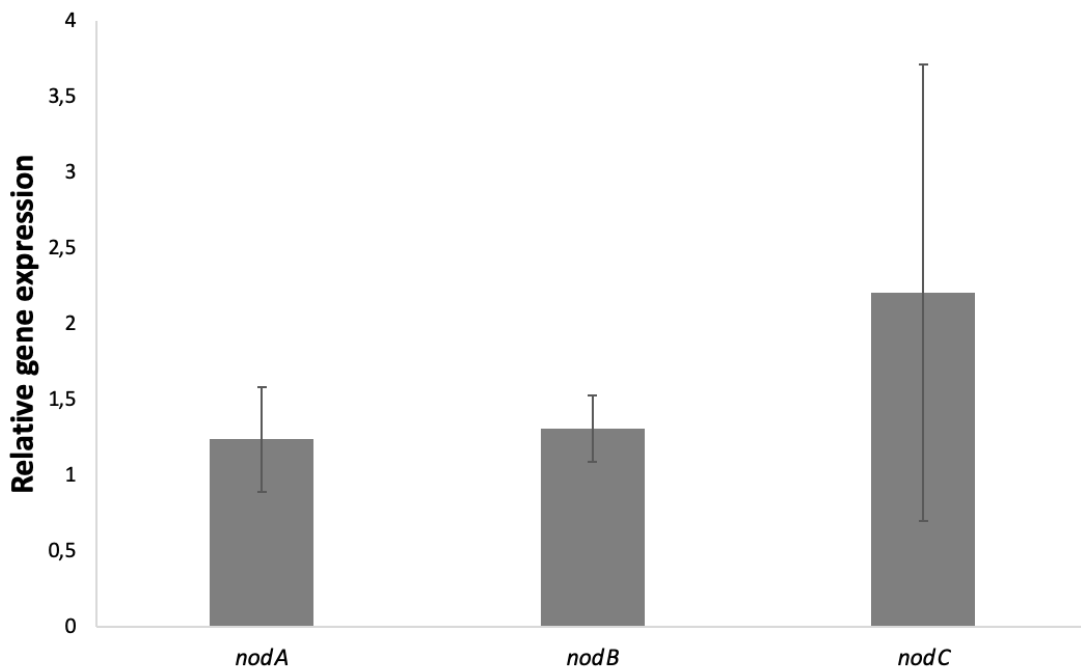


1072

1073 Figure 5. Expression of the *pnodB*<sub>19424</sub>-*lacZ* fusion in *Cupriavidus taiwanensis*  
 1074 LMG19424, *Cupriavidus necator* UYPR2.512, and *Cupriavidus* sp. UYMMa02A  
 1075 in response to *Mimosa magentea* root exudates (RE).

1076

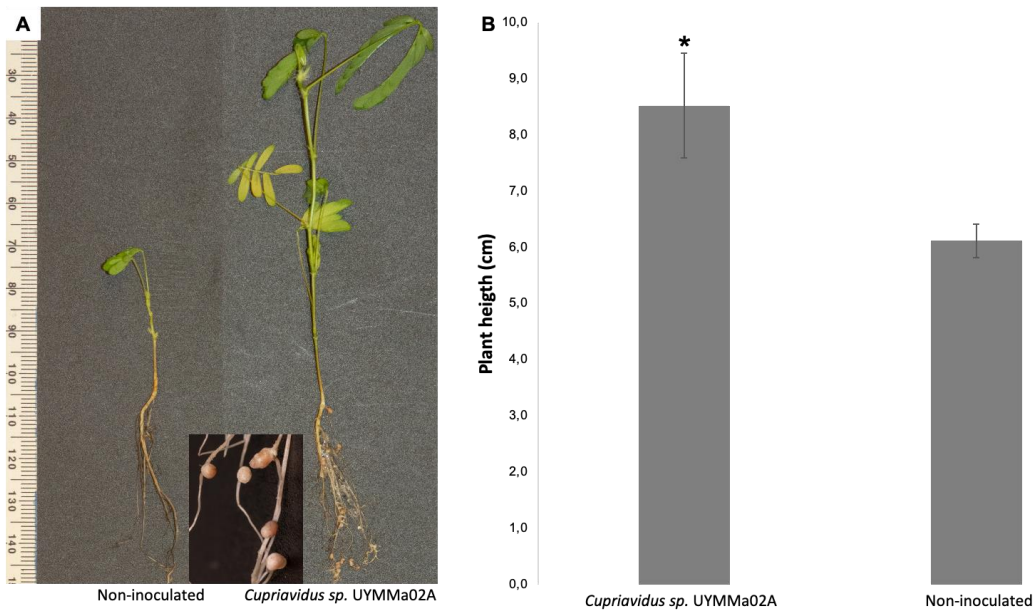
1077



1078

1079 Figure 6: UYMMa02A *nodA*, *nodB*, and *nodC* expression in response to *M.*  
1080 *pudica* root exudates. The bars represent the relative expression (Fold Change)  
1081 of the *nodA*, *nodB*, and *nodC* genes to the housekeeping genes *elongation factor*  
1082 *G (efg)* and *ribosomal protein S14 (S14)* when growing in M9 media  
1083 supplemented with *M. pudica* root exudates versus in M9 media without  
1084 exudates.

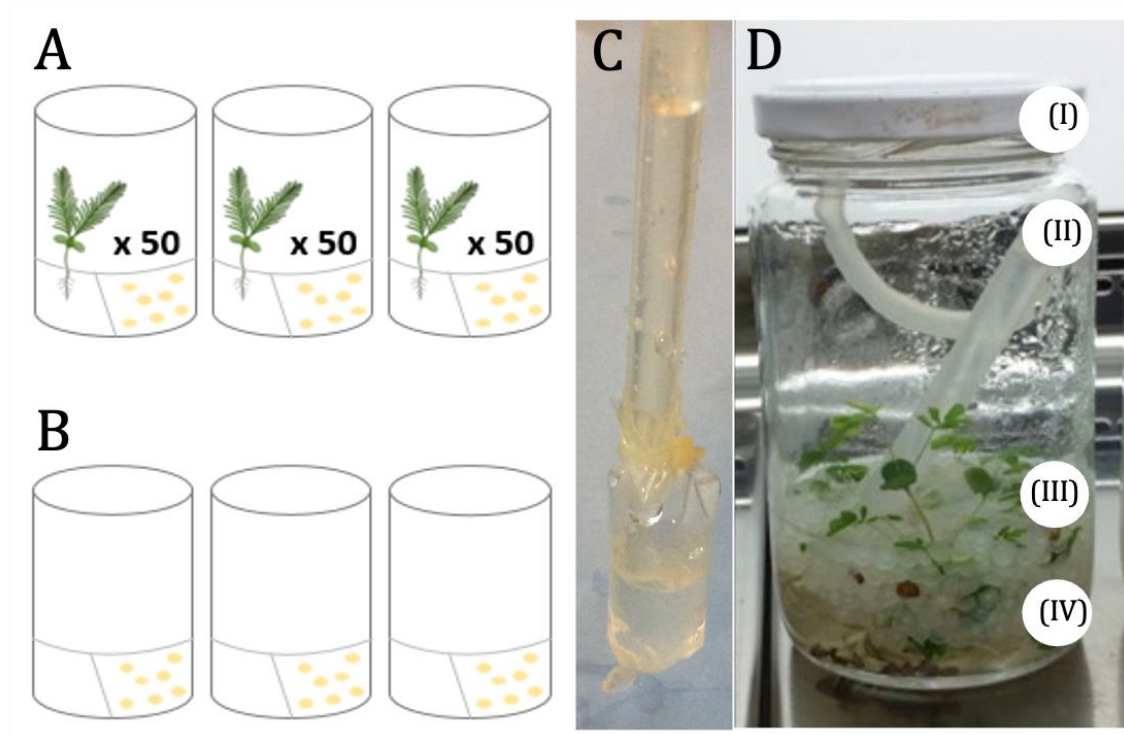
1085



1086  
1087 Figure 7: *Mimosa pudica* growth promotion ability of *Cupriavidus sp. UYMMa02A*.

1088 A. Examples of *M. pudica* development phenotype when inoculated with  
1089 *Cupriavidus sp. UYMMa02A* or not inoculated. Insert, detail of the nodules  
1090 formed by *Cupriavidus sp. UYMMa02A* in *M. pudica* roots. B. *M. pudica* plant  
1091 height was recorded 30 days post-inoculation with *Cupriavidus sp. UYMMa02A*  
1092 or with water as non-inoculated control. Asterisk indicates significant differences  
1093 (p-value < 0.01) between inoculated plants and non-inoculated plants.

1094

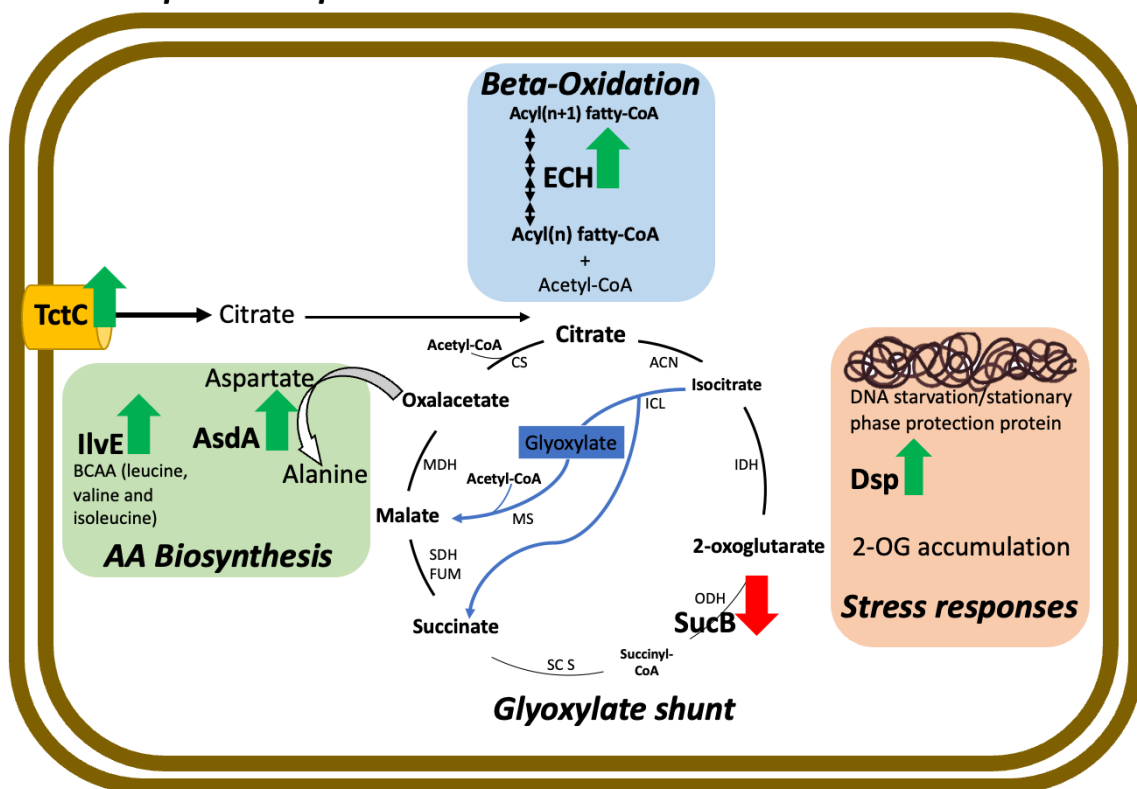


1095

1096 Figure 8. Plant-microorganism co-culture system. Bacteria were grown in the  
 1097 presence (A) or absence (B) of *M. pudica* plants. To prevent direct physical  
 1098 interaction between symbionts, the bacteria were placed inside a membrane  
 1099 tubing (C). D. Picture of the real co-culture assembled system (I) jar lid; (II)  
 1100 silicone tube connected to the membrane for bacterial inoculation; (III) *M. pudica*  
 1101 plants; (IV) Mineral plant culture medium containing polypropylene balls for  
 1102 seedling support. As control treatments, plant-free systems were used (B).

1103

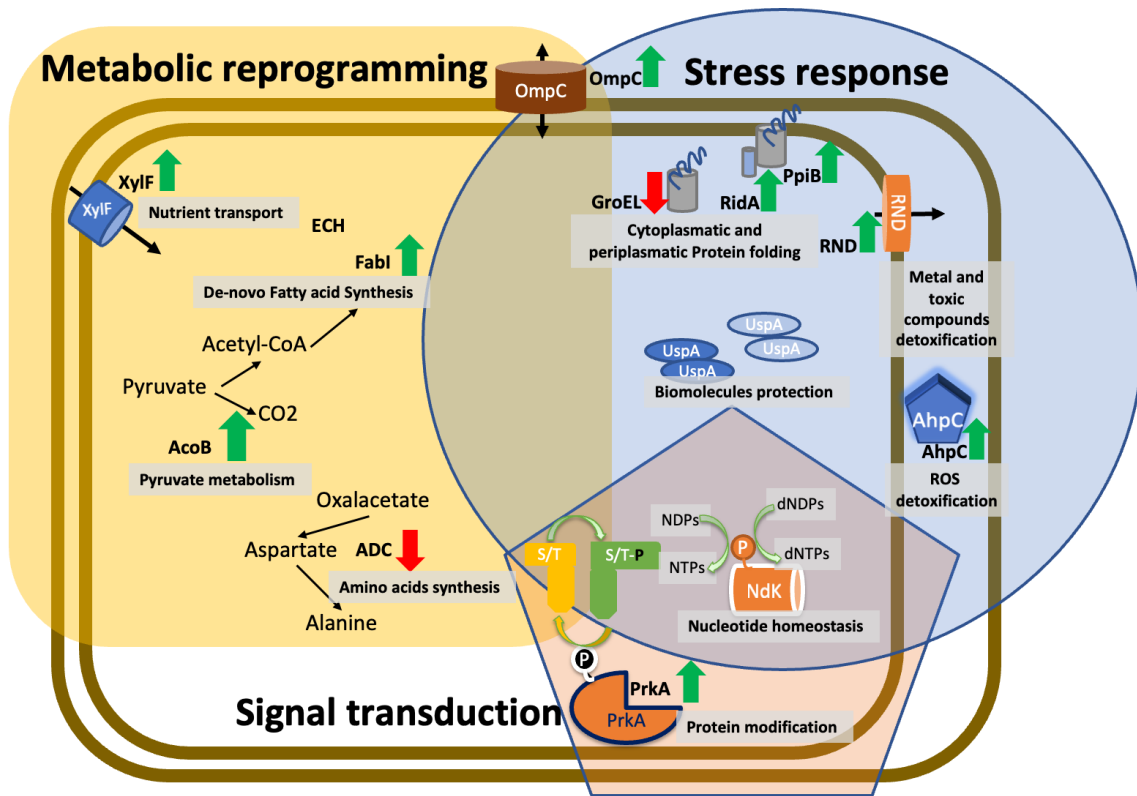
*Cupriavidus* sp. UYMMa02A-Flavonoids



1104

1105 Figure 9. UYMMa02A proteins and pathways observed in response to flavonoids.  
 1106 Proteins differentially expressed in the presence of apigenin and/or luteolin are  
 1107 highlighted in bold. Green and red arrows indicate if proteins were found either  
 1108 upregulated (up direction) or downregulated (down direction), with respect to the  
 1109 control condition. The main cellular processes affected are indicated in bold and  
 1110 cursive text. See the text for a full description.

1111



1112

1113 Figure 10. Model for the proteomics response of *Cupriavidus sp.* UYMMa02A-  
 1114 *Mimosa pudica* co-culture treatment. The illustration shows the main metabolic  
 1115 pathway, biological functions, chemical reactions, enzymes, and other proteins  
 1116 regulated in *Cupriavidus sp.* UYMMa02A grown in a co-culture system with the  
 1117 plant host *M. pudica*. Green and red arrows indicate proteins either upregulated  
 1118 (up direction) or downregulated (down direction) with respect to the control  
 1119 condition. Metabolic pathways affected are shadowed in grey. Color shadows  
 1120 were used to cluster affected proteins according to cellular processes; Metabolic  
 1121 reprogramming (in yellow), Stress response (in blue), and Signal transduction (in  
 1122 orange). Proteins implicated in more than one cellular process have been  
 1123 included at shadow intersections. See the text for a full description.

1124



1125 Table 1. Strains and plasmids used in this work

Strain	Relevant Characteristics	Reference
<i>Escherichia coli</i> DH5 $\alpha$	Cloning host; F <sup>-</sup> $\lambda^-$ <i>endA1 glnX44(AS) thiE1 recA1 relA1 spoT1 gyrA96(Nal<sup>R</sup>) rfbC1 deoR nupG <math>\Phi</math>80(lacZ<math>\Delta</math>M15) <math>\Delta</math>(argF-lac)169 hsdR17.</i>	(Hanahan, 1983)
<i>Cupriavidus sp.</i> UYMMa02A	Wild-type strain, isolated from <i>Mimosa magentea</i> nodules in Uruguay.	(Platero, et al., 2016)
<i>Cupriavidus taiwanensis</i> LMG19424 <sup>T</sup>	Type strain. Isolated from <i>Mimosa pigra</i> nodules in Taiwan.	(Chen et al., 2001)
<i>Cupriavidus necator</i> UYPR2.512	Wild-type strain, isolated from <i>Parapiptadenia rigida</i> nodules in Uruguay.	(Taulé et al., 2012)
Plasmid	Relevant characteristics	Reference
pRK600	Helper plasmid used for conjugation, Cf <sup>R</sup>	(Kessler et al., 1992)
pCZ388	pLAFR6 derivative containing a promoterless <i>lacZ</i> gene, Tc <sup>R</sup>	(Cunnac et al., 2004)
pCBM01	pCZ388 containing 401 bp of the <i>Cupriavidus taiwanensis</i> LMG19424 <i>nodB</i> promoter, Tc <sup>R</sup>	(Marchetti, et al., 2010)

1126

1127

1128 Table 2. *Cupriavidus* sp. UYMMa02A proteins differentially expressed in the  
 1129 presence of apigenin and luteolin

Spot	Fold change	p-value	Mascot score	Sequence coverage (%)	IP	MW (KDa)	Identified protein		COG category	Localization
							Protein name	ID		
<b>Apigenin induced proteins</b>										
103	1,5	0,019	163	18	5,5	60,8	Bifunctional aspartate transaminase/aspartate 4-decarboxylase	<a href="#">WP_224080690.1</a>	E	Cytoplasmic
272	1,4	0,027	185	38	5,8	27,9	Enoyl-CoA hydratase	<a href="#">ODV41316.1</a>	I	Cytoplasmic
257	1,5	0,004	157	16	9,6	33,4	Tripartite tricarboxylate transporter substrate binding protein	<a href="#">WP_011299555.1</a>	C	Periplasmic
224	1,5	0,052	157	33	5,9	39,4	Branched chain amino acid aminotransferase	<a href="#">ODV41908.1</a>	E	Cytoplasmic
<b>Luteolin induced proteins</b>										
103	1,5	0,050	163	18	6	60,8	Bifunctional aspartate transaminase/aspartate 4-decarboxylase	<a href="#">WP_224080690.1</a>	E	Cytoplasmic
317	1,4	0,021	94	44	6	18,2	DNA starvation/stationary phase protection protein	<a href="#">WP_211952485.1</a>	P	Cytoplasmic
335	3,4	0,001	239	33	6	55	Aldehyde dehydrogenase	<a href="#">ODV42183.1</a>	C	Cytoplasmic
<b>Apigenin repressed proteins</b>										
155	1,4	0,002	143	36	9	32,1	E2 component of the 2-oxoglutarate dehydrogenase complex	<a href="#">WP_211945176.1</a>	C	Cytoplasmic

1130

1131

1132 Table 3. Proteins differentially expressed during *Cupriavidus sp.* and *Mimosa*

1133 *pubida* co-cultures

Spot	Fold change	p-value	Mascot score	Sequence coverage (%)	IP	MW (KDa)	Identified protein		COG category	Localization
							Protein Name	ID		
<b>Induced proteins</b>										
507	1,5	0,029	147	27	6,1	15,3	Nucleoside-diphosphate kinase Ndk	WP_211957553.1	F	Cytoplasmic / Extracellular
629	1,8	0,036	181	40	9,3	32,1	ABC transporter, substrate-binding protein XylF	ODV42702.1	G	Extracellular / Cytoplasmic
292	2,4	0,005	109	13	9	42,2	Outer membrane protein Porin	WP_224081450.1	M	Outer membrane
308	2,3	0,041	111	39	5,2	36	Acetoin dehydrogenase E1 component beta-subunit	WP_220630611.1	-	Cytoplasmic
357	1,2	0,026	348	28	5,6	27,5	enoyl-ACP reductase FabI	WP_211945097.1	I	Cytoplasmic/ Periplasmic
391	1,8	0,034	184	51	6,2	24,1	Peroxiredoxin	WP_211946599.1	O	Periplasmic
499	1,5	0,035	74	12	5,9	16,2	RidA family protein	WP_211958671.1	J	Cytoplasmic
462	1,3	0,041	352	66	5,7	18,1	Cyclophilin/peptidylprolyl isomerase	ODV42271.1	O	Cytoplasmic
199	1,5	0,004	251	37	6,2	43,3	Efflux RND periplasmic adaptor subunit	ODV41844.1	P	Periplasmic
361	1,3	0,007	126	28	7	27,6	Enoyl-CoA hydratase	ODV41316.1	Q	Cytoplasmic
528	1,4	0,036	237	65	6,3	15,2	Universal stress protein UspA	WP_071013637.1	T	Extracellular / Cytoplasmic
512	1,3	0,002	156	18	5,2	15,8	Universal stress protein UspA	ODV41046.1	T	Extracellular / Cytoplasmic
78	1,7	0,013	216	52	5,5	73,4	Serine protein kinase PrkA	ODV43245.1	T	Cytoplasmic
74	1,7	0,027	130	19	5,5	73,4	Serine protein kinase PrkA	ODV43245.1	T	Cytoplasmic
<b>Repressed proteins</b>										
106	1,3	0,03	163	18	5,5	60,8	Bifunctional aspartate transaminase/aspartate 4-decarboxylase	WP_011298857.1	E	Cytoplasmic
113	2,7	0,01	221	37	8,4	62,5	PPQ-dependent dehydrogenase	WP_224007080.1	G	Periplasmic
625	1,4	0,047	459	42	5,1	57,3	Chaperonin GroEL	WP_035877914.1	O	Cytoplasmic

1134

1 **Nodulation in absence of *nod* genes induction: alternative mechanisms**  
2 **involved in the symbiotic interaction between *Cupriavidus* sp. UYMMa02A**  
3 **and *Mimosa pudica***

4 Cecilia Rodríguez-Esperón<sup>1+</sup>, Laura Sandes<sup>1+</sup>, Ignacio Eastman<sup>1</sup>, Carolina  
5 Croci<sup>1,2</sup>, Florencia Garabato<sup>1</sup>, Virginia Ferreira<sup>1</sup>, Martín Baraibar<sup>3</sup>, Magdalena  
6 Portela<sup>4,5</sup>, Rosario Durán<sup>4</sup>, and Raúl A. Platero<sup>1\*</sup>

7 **Affiliations:** <sup>1</sup>Laboratorio de Microbiología Ambiental. Departamento de  
8 Bioquímica y Genómica Microbianas, Instituto de Investigaciones Biológicas  
9 Clemente Estable, Ministerio de Educación y Cultura, Uruguay <sup>2</sup>Current  
10 affiliation: Laboratorio de Ecología Microbiana Acuática, Departamento de  
11 Microbiología, Instituto de Investigaciones Biológicas Clemente Estable,  
12 Ministerio de Educación y Cultura, Uruguay. <sup>3</sup>OXIProteomics, France. <sup>4</sup>Unidad  
13 Mixta de Bioquímica y Proteómica Analíticas, Institut Pasteur de Montevideo-  
14 Instituto de Investigaciones Biológicas Clemente Estable, Ministerio de  
15 Educación y Cultura, Uruguay. <sup>5</sup>Facultad de Ciencias, Universidad de la  
16 República, Uruguay.

17 \*Corresponding author: Raúl A. Platero [rplatero@iibce.edu.uy](mailto:rplatero@iibce.edu.uy)

18 +These authors contributed equally to the present work

19 Keywords: Beta-rhizobia, *Cupriavidus*, luteolin, apigenin, proteomic, 2D-DIGE,  
20 *Mimosa pudica*, *Mimosa magentea*, root exudates

21 **Abstract:** *Cupriavidus* sp. UYMMa02A is a beta-rhizobia strain of the  
22 *Cupriavidus* genus isolated from nodules of *Mimosa magentea* in Uruguay. This

23 strain can form effective nodules with several *Mimosa* species, including its  
24 original host. Genome analyses indicated that *Cupriavidus* sp. UYMMa02A strain  
25 has a highly conserved 35kb symbiotic island containing *nod*, *nif* and *fix* operons,  
26 suggesting conserved mechanisms for the symbiotic interaction with plant hosts.  
27 However, *Cupriavidus* sp. UYMMa02A produces functional nodules and  
28 promotes *Mimosa pudica* growth under nitrogen-limiting conditions, but *nod*  
29 genes were not induced by luteolin or *Mimosa spp.* root exudates exposure. To  
30 explore alternative mechanisms implicated in the *Cupriavidus-Mimosa*  
31 interaction, we assessed the proteomic profiles of *Cupriavidus* sp. UYMMa02A  
32 grown in the presence of pure flavonoids and co-culture with *Mimosa pudica*  
33 plants. This approach allows us to identify 24 differentially expressed proteins  
34 potentially involved in bacterial-plant interaction. A possible model for *nod*-  
35 alternative symbiotic interaction is proposed in light of the obtained results.